

The Effect of the Angle of Perforation on Inserts in a Pipe Flow for Heat Transfer Analysis



By

Simul Acherjee
ID. 17MMATH003P

A thesis submitted in partial fulfillment of the
requirements for the degree of
MASTER of PHILOSOPHY in MATHEMATICS

Department of Mathematics
CHITTAGONG UNIVERSITY OF ENGINEERING
& TECHNOLOGY
JUNE 2024

Similarity Report Summary on the Thesis

Title: The Effect of the Angle of Perforation on Inserts in a Pipe Flow for Heat Transfer Analysis

Student Name : Simul Acherjee
Student ID : 17MMATH003P

Overall Similarity : 33%
Individual Source Similarity : < 1% (Except Sources 1, 2,3, and 4)
Primary Sources 1 : 14% (It is a published paper of the Author and included in the Thesis as it is in **Chapter 2, 3, 4 and 5**)
Primary Sources 2 : 2%
Primary Sources 3 : 1%
Primary Sources 4 : 1%
Finally, the similarity index of the Thesis : 33% - 14% (Primary **Sources 1**) = 19%

Note: The report is attached herewith.

(Professor Dr. Ujjwal Kumar Deb)
Supervisor of the M. phil. Student
Simul Acherjee
ID. 17MMATH003P
Department of Mathematics
Chittagong University of Engineering & Technology (CUET)

1

The Effect of the Angle of Perforation on Inserts in a Pipe Flow for Heat Transfer Analysis



By

Simul Acherjee

ID. 17MMATH003P

49

A thesis submitted in partial fulfillment of the requirements
for the degree of

MASTER of PHILOSOPHY in MATHEMATICS

Department of Mathematics

**CHITTAGONG UNIVERSITY OF ENGINEERING
AND TECHNOLOGY**

JUN 2024

ORIGINALITY REPORT

33%

SIMILARITY INDEX

%

INTERNET SOURCES

33%

PUBLICATIONS

%

STUDENT PAPERS

PRIMARY SOURCES

1

Simul Acherjee, Ujjwal Kumar Deb, Md. Moniruzzaman Bhuyan. "The effect of the angle of perforation on perforated inserts in a pipe flow for heat transfer analysis", Mathematics and Computers in Simulation, 2020

Publication

14%

2

Giulio Lorenzini, Simone Moretti, Alessandra Conti. "Fin Shape Thermal Optimization Using Bejan's Constructal Theory", Springer Science and Business Media LLC, 2011

Publication

2%

3

Robert E. Masterson. "Nuclear Reactor Thermal Hydraulics - An Introduction to Nuclear Heat Transfer and Fluid Flow", CRC Press, 2019

Publication

1%

4

Yatish T. Shah. "Thermal Energy - Sources, Recovery, and Applications", CRC Press, 2018

Publication

1%

5

Md. Moniruzzaman Bhuyan, Ujjwal K. Deb, M. Shahriar, Simul Acherjee. "Simulation of Heat Transfer in a Tubular Pipe Using Different Twisted Tape Inserts", Open Journal of Fluid Dynamics, 2017

Publication

<1 %

6

Sujoy Kumar Saha, Manvendra Tiwari, Bengt Sundén, Zan Wu. "Advances in Heat Transfer Enhancement", Springer Science + Business Media, 2016

Publication

<1 %

7

Raj P. Chhabra. "CRC Handbook of Thermal Engineering Second Edition", CRC Press, 2017

Publication

<1 %

8

Bahman Zohuri, Nima Fathi. "Thermal-Hydraulic Analysis of Nuclear Reactors", Springer Science and Business Media LLC, 2015

Publication

<1 %

9

Anthony F. Mills. "Heat and Mass Transfer", CRC Press, 2018

Publication

<1 %

10

M. M. K. Bhuiya, J. U. Ahamed, M. A. R. Sarkar, B. Salam, A. S. M. Sayem, A. Rahman. "Performance of Turbulent Flow Heat Transfer Through a Tube With Perforated

<1 %

132	William S. Janna. "Introduction to Fluid Mechanics", CRC Press, 2019	<1 %
Publication		

133	Yeong Koo Yeo. "Chemical Engineering Computation with MATLAB®", CRC Press, 2020	<1 %
Publication		

134	Zhen Liu. "Chapter 3 How to Do Multiphysics", Springer Science and Business Media LLC, 2018	<1 %
Publication		

Exclude quotes	Off
Exclude bibliography	Off

Exclude matches	Off
-----------------	-----

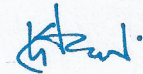
CERTIFICATION

The thesis titled “**The Effect of the Angle of Perforation on Inserts in a Pipe flow for Heat Transfer Analysis**” submitted by Simul Acherjee, Roll No.: 17MMATH003P, Session 2017-2018 has been accepted as satisfactory in partial fulfillment of the requirement for the degree of Master of Philosophy on June 30, 2024.

BOARD OF EXAMINERS

Supervisor

1. (Prof. Dr. Ujjwal Kumar Deb)
Department of Mathematics
Chittagong University of Engineering & Technology
Chittagong-4349, Bangladesh.



Chairman

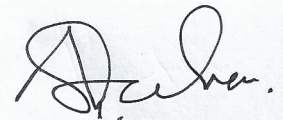
Head

2. (Prof. Dr. Musammet Tahmina Akter)
Department of Mathematics
Chittagong University of Engineering & Technology
Chittagong-4349, Bangladesh.



Member

3. Prof. Dr. Ashutose Saha
Department of Mathematics
Chittagong University of Engineering & Technology
Chittagong-4349, Bangladesh.



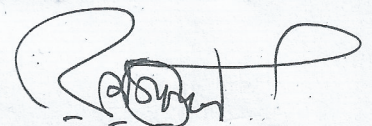
Member

4. Prof. Dr. Mohammad Shah Alam
Department of Mathematics
Chittagong University of Engineering & Technology.



Member

5. Prof. Dr. Rabindra Nath Mondol
Department of Mathematics
Jagannath University



Member (External)

Declaration

I hereby declare that the work contained in this Thesis has not been previously submitted to meet requirements for an award at this or any other higher education institution. To the best of my knowledge and belief, the Thesis contains no material previously published or written by another person except where due reference is cited. Furthermore, the Thesis complies with the PLAGIARISM and ACADEMIC INTEGRITY regulation of CUET.

Student Name: **Simul Acherjee**

Student ID: 17MMATH 003P

Department of Mathematics

Chittagong University of Engineering & Technology (CUET)

Copywrite © Simul Acherjee 2024.

This work may not be copied without permission of the author or Chittagong University of Engineering & Technology (CUET).

Dedication

To

My Family members and All of My Honorable Teachers

List of Publications

Published Paper:

The results presented in the following publications are included in this thesis.

1. **Simul Acherjee**, Ujjwal Kumar Deb, Md. Moniruzzaman Bhuyan, The effect of the angle of perforation on perforated inserts in a pipe flow for heat transfer analysis, *Mathematics and Computers in Simulation* 171 (2020) 306–314, <https://doi.org/10.1016/j.matcom.2019.10.003> Published by Elsevier. **(Chapter 2, 3, 4 and 5).**

Approval/Declaration by the Supervisor

This is to certify that **Simul Acherjee** has carried out this research work under my supervision, and that he has fulfilled the relevant Academic Ordinance of the Chittagong University of Engineering & Technology, so that he is qualified to submit the following Thesis in the application for the degree of MASTER of PHILOSOPHY in Mathematics. Moreover, the Thesis complies with the PLAGIARISM and ACADEMIC INTEGRITY regulation of CUET.

Supervisor Name: **Dr. Ujjwal Kumar Deb**

Designation: Professor

Department of Mathematics

Chittagong University of Engineering & Technology (CUET)

Acknowledgement

At first I thanks to the God for giving me a chance to do this research work and giving me the strength and ability to successfully completion of this research work.

It is my pleasure to express my heartfelt thanks and deep sense of respect to my supervisor **Dr. Ujjwal Kumar Deb**, Professor, Department of Mathematics, Chittagong University of Engineering & Technology (CUET) for his kind supervision, constant help, and valuable suggestions and also for all kinds of supports during this thesis work. It was really nice to work with him.

I am grateful to **Prof. Dr. Musammet Tahamina Akter**, Head of the Department of mathematics and **Prof. Dr. Mohammad Shah Alam**, Department of Mathematics, CUET for their openhanded and warm co-operations to accomplish this research work.

I would like to express my cordial thanks to all of my teachers of the Department of Mathematics, CUET for their valuable suggestions and excellent supports during the entire period of this work.

I acknowledge my gratitude through my respected supervisor to the Centre of Excellence in Mathematics, Dept. of Mathematics, Mahidul University, Bangkok-10400, Thailand, and also my gratitude to the Simulation Lab, Department of Mathematics, and CUET for the technical supports to accomplish this research work.

I am extremely thankful to the authority of Chittagong University of Engineering & Technology (CUET) for all kinds of support during this thesis work.

Finally I am indebted to my family members for their constant inspiration and supports during this work. I would like to thank all of my colleagues, relatives, friends and well-wisher's for their cordial help and encouragement.

The Author

Abstract

A numerical simulation study of heat transfer analysis is considered with perforated inserts using a different angle of perforation in a circular pipe. In our simulation, we have used 0° , 5° , 10° , 15° , 16° , 17° , 20° , 30° , 40° , 50° , 60° , 65° , 68° and 70° angles of perforation respectively in a perforated axial insert considering the non-isothermal laminar flow. The inserts are used perpendicular to the fluid flow inside a pipe. A uniform heat-flux around the circular tube is assumed for our simulations. The temperature and pressure distribution are measured for a different angle of perforation. The relation between heat transfer rate and wall temperature is observed and found that the heat transfer rate increases inversely with the wall temperature. The effect of Nusselt number and friction factor are the diagnosis for all including angles and Reynolds numbers. The Thermal Performance Evaluation Criterion (PEC) is also analyzed in this study.

বিমূর্ত

একটি বৃত্তাকার পাইপের ভিতর ছিদ্রযুক্ত সন্নিবেশে ছিদ্রের বিভিন্ন কোণের জন্য তাপ স্থানান্তর বিশ্লেষণের একটি সংখ্যাসূচক সিমুলেশন অধ্যয়ন করা হয় এ গবেষণায়। আমাদের সিমুলেশনে একটি ছিদ্রযুক্ত অক্ষীয় সন্নিবেশে যথাক্রমে 0° , 5° , 10° , 15° , 16° , 17° , 20° , 30° , 40° , 50° , 60° , 65° , 68° এবং 70° ছিদ্রের কোণ ব্যবহার করা হয় একটি নন-আইসোথার্মাল ল্যামিনার প্রবাহ বিবেচনা করে। উল্লেখ্য যে, সন্নিবেশগুলি একটি পাইপের ভিতরে তরলের প্রবাহের সাথে লম্বভাবে স্থাপন করা হয়। আমাদের সিমুলেশনের জন্য বৃত্তাকার টিউবের চারপাশে একটি অভিন্ন তাপ-প্রবাহ অনুমান করা হয়। ছিদ্রের ভিন্ন ভিন্ন কোণের জন্য তাপমাত্রা এবং চাপ বন্টন পরিমাপ করা হয়। পাশাপাশি তাপ স্থানান্তর হার এবং দেওয়ালের তাপমাত্রার মধ্যে সম্পর্ক পর্যবেক্ষণ করা হয় এবং লক্ষ করা যায় যে তাপ স্থানান্তর হার দেওয়ালের তাপমাত্রার সাথে বিপরীতক্রমে বৃদ্ধি পেতে থাকে। ন্যূনতম সংখ্যা এবং ঘর্ষণ ফ্যাক্টরের প্রভাবে, কোণ এবং রেনল্ডস সংখ্যার কি পরিবর্তন হয় তা এখানে নির্ণয় করা হয়। থার্মাল পারফরমেন্স ইন্ডেক্স (TEFI) ও এই গবেষণায় বিশ্লেষণ করা হয়েছে।

Table of Contents

Abstract		vii
বিমূর্ত		viii
Table of Contents		ix
List of Figures		xi
List of Tables		xiii
Nomenclature		xiv
Chapter 1	Introduction	1
	1.1 General overview	1
	1.2 Objectives with specific aims and possible outcomes	2
	1.3 Thesis outlines	2
Chapter 2	Literature Review	4
	2.1 Introduction	4
	2.2 Fluid	5
	2.2.1 What is Fluid?	5
	2.2.2 Properties of Fluids	5
	2.2.3 Viscosity	7
	2.2.4 Reynolds Number (Re)	8
	2.2.5 Laminar and Turbulent Flow	9
	2.2.5.1 Laminar Flow	9
	2.2.5.2 Turbulent Flow	10
	2.2.6 Flow in a Circular Tube	10
	2.3 Heat Transfer	11
	2.3.1 What is Heat Transfer?	11
	2.3.3 Hydraulic Diameter(D)	12
	2.3.3 Average Wall Temperature (T_w)	12
	2.3.4 Bulk Temperature/ Average Fluid Temperature (T_b)	13
	2.3.5 Thermal Conductivity (k)	13
	2.3.6 Heat Transfer rate (Q)	14
	2.3.7 Heat Transfer Coefficient (h)	14
	2.3.8 Nussalt Number (Nu)	15
	2.3.9 Pressure Drop (ΔP)	15
	2.3.10 Friction Factor (f)	16
	2.4 Heat Exchanger	16
	2.4.1 What is Heat Exchanger?	16
	2.4.2 Classification of Heat Exchangers	17

	2.4.3 Porosities (R_p)	18
	2.5 Computational Methods	19
	2.5.1 Finite difference Method	19
	2.5.2 Finite Volume Method	19
	2.5.3 Boundary Element Method	20
	2.5.4 Finite Element Method	20
	2.6 Computational Fluid Dynamics	20
	2.7 Previous Studies	22
Chapter 3	Mathematical Model and Computational Domain	27
	3.1 Conservation of Fluid and Heat Transfer Equations	27
	3.1.1 The Control Volume	27
	3.1.2 The Partial Time Derivative $\partial B/\partial t$	28
	3.1.3 Total Time Derivative DB/dt	28
	3.1.4 Substantial time derivative DB/Dt	28
	3.2 Continuity Equation	29
	3.3 Equation of motion	31
	3.4 Energy Equation	32
	3.5 Governing Equations for Simulation	34
	3.6 Boundary Conditions	36
	3.7 Computational domain	37
	3.8 Mesh generation	39
Chapter 4	Results and discussion	41
	4.1 Introduction	41
	4.2 Velocity profile analysis	41
	4.3 Temperature Augmentation Assessment	43
	4.4 Wall temperature and Bulk temperature analysis	45
	4.5 Heat transfer coefficient analysis	49
	4.6 Wall temperature and Heat transfer coefficient relation	50
	4.7 Nusselt number Performance Evaluation	51
	4.8 Nusselt number and Heat transfer coefficient relation	52
	4.9 Streamline phenomena	53
	4.10 Pressure drop distribution	54
	4.11 Friction Factor Performance Evaluation	56
	4.12 Friction Factor and Pressure drop relation	57
	4.13 Thermal Performance Criterion	58
Chapter 5	Conclusion and Recommendations	60
	5.1 Conclusion	60
	5.2 Recommendation for future work	61
References		62

List of Figures

Figure No.	Figure Caption	Page No.
Figure 2.1	Flow of fluid.	5
Figure 2.2	Laminar and turbulent flow of fluid.	8
Figure 2.3	Laminar, Transition and turbulent boundary layer flow regimes in flow over a flat plate.	10
Figure 2.4	Laminar and turbulent flow velocity profiles.	10
Figure 2.5	Heat transfer in a solid.	11
Figure 2.6	Heat conduction, Convection and Radiation.	12
Figure 2.7	Types of heat exchanger.	16
Figure 2.8	Classification of heat exchangers.	18
Figure 3.1	Coordinate systems (a) Rectangular, (b) Cylindrical, (c) Spherical.	27
Figure 3.2	Differential volume element in three dimension.	29
Figure 3.3	The angle orientation of rectangular strips inserts of the perforation angle of 0° , 30° , 65° and 70° .	37
Figure 3.4	The angles of perforation 0° , 5° , 10° , 15° , 16° , 17° , 20° , 30° , 40° , 50° , 60° , 65° , 68° and 70° respectively.	38
Figure 3.5	The computational domain of angle oriented perforated inserts U-loop pipe.	38
Figure 3.6	Meshing of the domain for (a) 0° angle oriented Perforated inserts tube (b) 30° angle oriented Perforated inserts tube (c) 65° angle oriented Perforated inserts tube.	39
Figure 4.1	Velocity profile of the fluid for (a) 0° angle oriented Perforated inserts tube (b) 30° angle oriented Perforated inserts tube (c) 65° angle oriented Perforated inserts tube (d) 70° angle oriented Perforated inserts tube.	42
Figure 4.2	Surface temperature and temperature line graph of the fluid for (a) 0° angle oriented Perforated inserts tube (b) 30° angle oriented Perforated inserts tube (c) 65° angle oriented Perforated inserts tube (d) 70° angle oriented Perforated inserts tube.	44
Figure 4.3	Bulk temperature phenomena of the fluid for (a) 0° angle oriented Perforated inserts tube (b) 30° angle oriented Perforated inserts tube (c) 65° angle oriented Perforated inserts tube (d) 70° angle oriented Perforated inserts tube.	45
Figure 4.4	Wall temperature graph of the fluid at different angle oriented inserts for different Reynolds number.	46
Figure 4.5	Variation of bulk temperature at different angle oriented inserts for different Reynolds number.	48
Figure 4.6	Variation of heat transfer coefficient at different angle	49

	oriented inserts for different Reynolds number.	
Figure 4.7	The comparison of wall temperature and heat transfer coefficient for the different angle of perforation	50
Figure 4.8	Nusselt number variation with Reynolds number for the different angle of perforation.	51
Figure 4.9	Nusselt number and heat transfer relation for the different angle of perforation.	52
Figure 4.10	Streamline phenomena of the fluid for (a) 68° angle oriented Perforated inserts tube (b) 65° angle oriented perforated inserts tube (c) 70° angle oriented perforated inserts tube.	54
Figure 4.11	Pressure drop distribution of the fluid at different angle oriented inserts for different Reynolds number.	55
Figure 4.12	Friction factor variation with Reynolds number for the different angle of perforation.	56
Figure 4.13	Friction factor and pressure drop relation for the different angle of perforation.	57
Figure 4.14	Thermal performance variation with Reynolds number for the different angle of perforation.	58

List of Tables

Table No.	Table Caption	Page No.
Table 3.1	Mesh element distribution for 65° angle oriented inserts fitted tube.	40
Table 4.1	Wall temperature data of the domain at different angle oriented inserts for different Reynolds number.	47
Table 4.2	Bulk temperature data of the domain at different angle oriented inserts for different Reynolds number.	48
Table 4.3	Heat transfer coefficient data of the domain at different angle oriented inserts for different Reynolds number.	50
Table 4.4	The comparison of wall temperature and heat transfer coefficient for the different angle of perforation.	51
Table 4.5	Nusselt number data of the domain at different angle oriented inserts for different Reynolds number.	52
Table 4.6	Nusselt number and heat transfer relation data for the different angle of perforation.	53
Table 4.7	Pressure drop distribution data of the fluid at different angle oriented inserts for different Reynolds number.	55
Table 4.8	Friction factor variation data with Reynolds number for the different angle of perforation.	56
Table 4.9	Friction factor and pressure drop relation for the different angle of perforation.	57
Table 4.10	Data of thermal performance variation with Reynolds number for the different angle of perforation.	58

Nomenclature

Symbol	Identity
ρ	Density (SI Unit: Kg/m^3)
\mathbf{u}	Velocity (SI: Unit m/s)
K	Thermal conductivity
Q	Amount of heat (SI: W/m^3)
q	Heat flux by conduction (SI: W/m^2)
T	Absolute Temperature (SI: K)
p	Pressure (SI: Unit pa)
τ	Viscous stress tensor (SI: Unit pa)
\mathbf{I}	Unit matrix
\mathbf{F}	Body force vector (SI: Unit N/m^3)
μ	Dynamic viscosity (Pa. s)
C_p	Specific heat capacity at constant pressure (SI: Unit J/Kg. K)
\mathbf{s}	Strain-rate tensor ($1/\text{s}$)
“ \cdot ”	The operation denotes a construction between tensors defined by

Chapter 1

Introduction

1.1 General overview

The exchange of heat between fluid to fluid or fluids and solid to fluid depends upon the properties of fluids, fluid flow behavior and heat exchanger devices. In this regards a well modified heat exchanger plays an important role in all kinds of mechanical and industrial sectors. So researchers need to improve the heat exchanger device using many special geometries. Some previous studies recommend that the heat transfer rate is proportional with the distance among the inserts for the rectangular box inserts in a circular pipe and for U-loop circular pipe ([Hossain *et al.* 2015](#), [Bhuyan *et al.* 2017](#)). For cut depth ($w = 0.5$ cm) and twist ratio ($y = 2.93$), the V-cut twisted tape insert enhanced 107% more than the other twisted tape inserts and the V-cut twisted tape insert. The study of ([Salman *et al.* 2013](#)) investigated a CFD inquiry and found that V-cut twisted tape inserts tubes for laminar flow. In order to explain the flow characteristic under various geometrical restrictions, a numerical study of the entire length of the of the twisted tape insert tube ([Bhattacharyya *et al.* 2014](#)) is conducted. [Bhuyan *et al.* \(2017\)](#) recommended extended-length twisted inserts because these type have shown better result than short-length twisted inserts.

According to [Suwannapan *et al.* \(2015\)](#), the Zigzag-Winglet perforated-tape (ZW-PT) insert demonstrates that the Pitch Ratio ($PR=1.0$) with the Blockage Ratio ($BR=0.15$) provides the superior Thermal Efficiency Factor (TEF) at the lowest Reynolds number. According to an experimental investigation ([Ahamed *et al.* 2007, 2011](#)) using perforated twisted inserts, the maximum quantity of heat was boosted by porosities of 4.6%. According to [Bhuiya *et al.* \(2013\)](#), in contrast to a plain tube, the 4.5% porosity increased the intense heat.

[Mizanuzzaman *et al.* \(2013\)](#) conducted an experimental investigation utilizing X-shaped axial perforated inserts for porosities of 5.7%, 10.15%, and 15.85%. The results suggested a greater efficiency for porosities of 15.85%. The ideal quantity of heat for perforated strip inserts is suggested by [Bhuiya *et al.* \(2012\)](#) to have porosities of 4.4% increased. However, the maximum heat enhancement was seen at porosities

of 4.42% for the axially perforated inserts fitted with U-loop pipe (Acherjee *et al.* 2017).

Laminar flow typically transfers more heat in heat transfer devices and increases the rate at which turns occur. The heat transmission rate at an optimal label is provided by the angle-oriented perforated inserts.

1.2 Objectives with specific aims and possible outcomes

From the above studies it is indicate that the perforated type inserts represent better performance than the plain type inserts. However there is no literature is found where the investigation done related to the effect of angle of perforation. For this we assume that this type of investigation helps us to understand about enhancement of heat transfer rate. A non-isothermal laminar flow will be chosen for the physics while water as acting fluid in our investigated simulation. This steady will be influence of angle of perforation on heat transfer rate and fluid flow performance and the results are compared with the perforated inserts tube and the plane tube. This will guided to compute the effect of angle of perforation on performance and evaluate the heat transfer augmentation and pressure drop.

Summarized objectives are given below:

- a) To study the heat transfer rate.
- b) To analyze the fluid flow behavior.
- c) To compare the results with regular perforated insert tube and angle oriented perforated inserts tube.

1.3 Thesis outlines

The rest of the thesis is ordered as follows:

Chapter II illustrates an overview on the fluid flow and heat transfer phenomena. Some basic concepts and important terminologies of finite element method and fluid flow and heat transfer are given as necessary. In this chapter, we also briefly discuss the literature reviews, which are related in our study.

In chapter III, A conservation model for heat transfer equations is established to understand the flow behavior and heat transfer augmentation. After that we analyze the computational domain formation and mesh configuration.

Then in chapter IV, We compute the numerical simulation for the domain using single phase laminar flow. The model is investigated with COMSOL MULTIPHYSICS version 4.2a simulation software. After that we discuss the variation of wall temperature, bulk temperature, heat transfer rate, Nuselt number, friction factor, and effectiveness by fourteen different angle oriented perforated strip inserts.

Finally, a brief discussion and conclusion for the entire study are contained in chapter V together with possible suggestions for future work that can lead to future development in this field.

Chapter 2

Literature Review

2.1 Introduction

Most of the mechanical systems in industrial sectors heat may absorb or enhanced out. In dryers, evaporators, furnaces, reaction vessels and distillation units fluid plays a vital role by heating or cooling. All the chases enhancing heat with flexible rate creates a major problem. Heat loss by the system is also need to put off in many cases.

The heat transfer in nature occurs in one or more of three different customs.

- I. Conduction**
- II. Convection**
- III. Radiation**

At the industrial region related with heat transfer fluid flow is an essential part for mechanical mechanisms. The properties and types of fluids frequently influence the enhancement of heat.

This chapter covers fluid properties, fluid flow behavior, heat transfer, and related topics such as friction factor, heat transfer coefficient, thermal conductivity, and heat transfer rate with constant heat flux. We also discussed some dimensionless number which are Reynolds number, Nusselts number and relation between them with their physical implication. After that we will discuss about the heat transfer device, porosities, computational methods etc. Then we conclude the chapter with the discussion about some related previous work.

2.2 Fluid

2.2.1 What is Fluid?



Figure 2.1: Flow of fluid.

Any material that deforms continuously due to a lack of rigid particle attachment is called a fluid. Under arbitrarily small shear stresses, common materials that emerge to "flow," such as flour, sugar, salt, many spices, etc., do not exhibit continuous deformation; while it is evident that these materials can be "transferred," their responses to shear stress are very different from fluid behavior.

2.2.2 Properties of Fluids

Fluids are classified by its properties and the physical behavior of any fluid is also estimated by them. The fluid properties can be expressed in two ways.

- I. General properties and
- II. Transport properties

Density, pressure, and temperature are the general attributes. Viscosity, thermal conductivity, and mass diffusivity are the transport qualities; all of these are also stated as thermodynamic properties, particularly when considering fluids. Finally, we also talk about surface tension.

Mass: The mass of a body is the total amount of matter that it contains. It is noted by m and the unit is kg .

Density: The relation between mass and volume is called density. It is measured as the mass per unit volume and is expressed as

$$\rho = \frac{m}{v}.$$

Where m is the mass of the volume v , and v is a finite volume of fluid. The dimension of density expresses by

$$\rho \sim M/L^3.$$

And the units is lbm/ft^3 .

The specific volume: A material's specific volume can be defined as its volume per mass unit. The specific volume is the inverse of density. The units of specific volume is ft^3/lbm . The density and the specific volume of the fluid are influenced by temperature and pressure. The density and the specific volume of the fluid both drop as its temperature rises.

The density and the specific volume of liquids remains unchanged with increasing in pressure because liquids are considered as incompressible. Liquids can, in fact, be somewhat compressed under high pressures, which causes a slight rise in density and a slight decrease in the liquid's specific volume.

The specific weight: The weight of a material per unit volume is its specific weight, γ . Since mass times acceleration equals weight, we know that weight is a force. Thus, the definition suggests

$$\gamma = \rho g,$$

where the acceleration caused by gravity is g . It is possible to substitute local acceleration caused by the spacecraft's tiny thrusters for the factor g in the event that analyzing the behavior of propellants in circling spacecraft tanks during station-keeping maneuvers is necessary. Keep in mind that since ρ represents mass per unit volume, γ must represent force per unit volume.

The specific weights dimension is,

$$\gamma \sim F/L^3.$$

In fluid dynamics, the ratio of specific heats is frequently represented by the symbol γ . In thermodynamics textbooks, C_p/C_v is typically represented by k .

A body's specific gravity is determined by dividing its weight by the weight of an equivalent volume of water at a specified temperature, typically 4 °C. Since it is a weight ratio, it lacks dimensions and units (McDonough, J. M. 2009).

Pressure: The definition of pressure in a fluid is force per unit area. Pounds of force per square inch, or psi, are commonly used to measure pressure.

$$\text{Pressure} = \frac{\text{Force}}{\text{Area}}$$

$$P = \frac{\text{Weight}}{\text{Area}}$$

$$P = \frac{mg}{Ag_c}$$

$$= \frac{\rho Vg}{Ag_c},$$

where A is the area in feet, V is the volume in feet, ρ is the fluid density in feet per unit of mass, g is the acceleration caused by earth's gravity in feet per second, and $g_c = 32.17 \text{ lbm-ft/lb-f sec}^2$.

By the collision of molecules with the walls of a circular tube, with inserts or with each other pressure arises at the molecular scales. From an engineering perspective, we can observe that in a hydrostatic scenario, pressure is created by the weight of the fluid. However, as we shall see later, fluid motion also contributes to pressure, as it is required to produce shear stresses. It would be noted that pressure in a gas always need to be in contact to a compressive force. Liquids, on the other hand, may withstand modest tensile forces in addition to absurd compressive normal forces. So, the pressure in a liquid may possible for it to be negative while pressure in a gas is always positive.

Temperature: This is the property of material which noticed a body how cold or hot. The direction of heat transfer can predict by temperature. The molecular vibration creates temperature in solid and liquid stage of matter, while the molecular translational motion for gas. For the fluid temperature depends on viscosity of fluids.

2.2.3 Viscosity (μ)

Viscosity is a property of fluid which indicates that the fluid particles do not slip past one another, or past the solid surfaces, very eagerly. It means the resistance of share stress. Viscosity is considered to measure the resistance of a fluid to flow. The

viscosity of water is low while it is high for thick oil. It denotes by μ and unit of viscosity is expresses m^2/s . The fluid's viscosity is influenced by its temperature. In most of the chases fluid temperature varies inversely with the fluid viscosity. For the lubricating oil of engines we observed that the oil is very viscous when it is cold but after started the engine the lubricating oil rises the temperature and the viscosity of the oil decreases radically.

2.2.4 Reynolds Number (Re)

In 1883, Osborne Reynolds arranged an experiment to explain the viscous flow phenomena for laminar and turbulent. In this experiment he was insert a dye with a thin stream into the water flow through a circular pipe. Then he observed that the dye stream moved with parallel layers in a noticeable straight path without any unsteady macroscopic mixing or capsizing movement of the layers for the low flow rates. This kind of flow is called laminar.

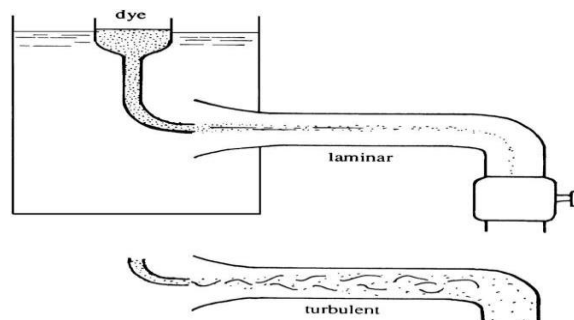


Figure 2.2: The Laminar and The turbulent flow of fluid (Pijush K. Kundu *et. al.* 2012).

On the other hand after increasing the flow rate at a certain critical value, a fluctuation occurs in dye stream line and the line turn into irregular string and spread all over the pipe with unsteady and chaotic three-dimensional macroscopic mixing motions. Thus kind of flow is called a turbulent.

The ratio of the inertia forces, which are the square of the fluid velocity and proportional to the fluid density, and viscous forces represent a fixed number that express the flow behavior is mentioned by his name, called Reynolds number.

$$\text{Reynolds number} = \frac{\text{inertia force}}{\text{viscous force}}$$

$$\text{Re} = \frac{\rho DV}{\mu},$$

where V is the average flow velocity (m/s), D is the diameter of pipe and μ is dynamic viscosity of the fluid (m^2/s). It is noted that the Reynolds number is a dimensionless number. By the Reynolds number we can conclude the flow is laminar or turbulent. The inertia forces are high comparatively with the viscous forces for the high Reynolds number. The arbitrary and quick variations of the fluid that give rise to turbulent flow are therefore unavoidable for the viscous forces. If there are sufficient viscous forces to control these variations and maintain the fluid's trajectory, the Reynolds number will drop to a small or moderate value.

The range of Reynolds number for circular pipe is given below:

$\text{Re} < 2300$	Laminar flow
$2300 < \text{Re} < 4000$	Transitional flow
$\text{Re} > 4000$	Turbulent flow

2.2.5 Laminar and Turbulent Flow

2.2.5.1 Laminar Flow

From the previous section we see that for the circular pipe if the Reynolds number below 2300 then the flow is laminar. In this case the streamline for the fluid particles never intersect each other that is the viscous forces control the fluid particles path line. Throughout the streamline, every fluid particle travels at a constant axial velocity, and for a fully developed laminar flow, the velocity profile $u(r)$ stays constant in the flow direction. Since there is no motion in the radial direction, there is no velocity component in the direction of the flow normal.

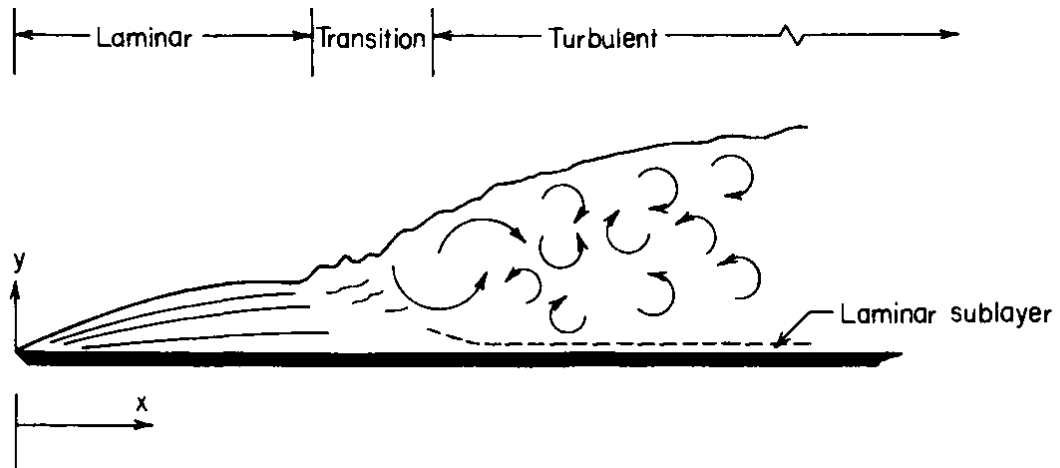


Figure 2.3: phases of boundary layer flow across a flat plate: Laminar, Transition, and Turbulent (Rohsenow *et.al.* 1998).

2.2.5.2 Turbulent Flow

Wavering of a laminar flow does not instantly lead to turbulence, which is a strictly nonlinear and chaotic flow state. The augmentation of small disturbances an initial breakdown of laminar flow occur and the flow go through a complex sequence of change, finally ensuing in the chaotic state we call turbulence. For the high Reynolds number greater than 4000 the flow turn into turbulence.

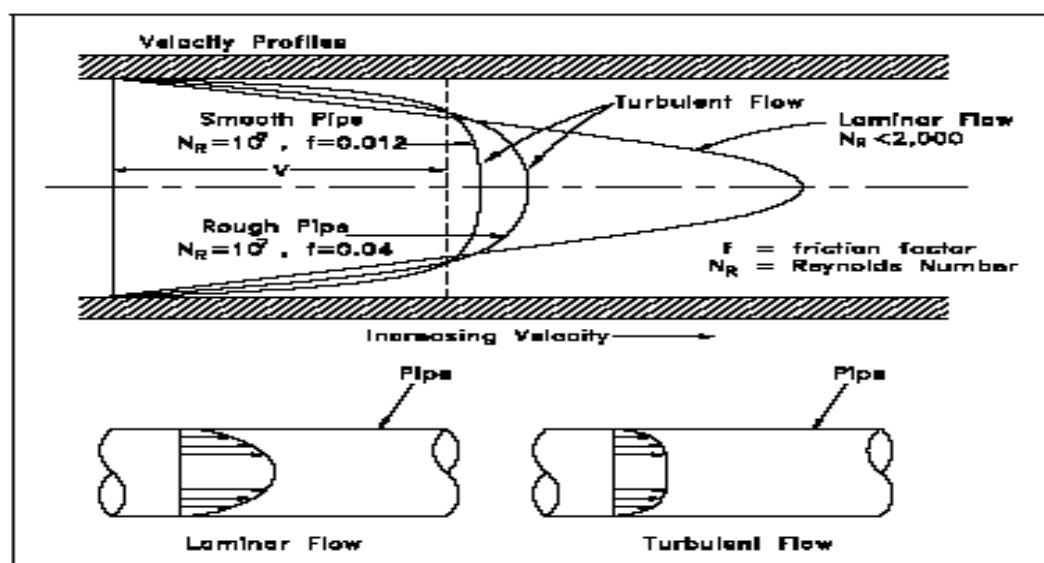


Figure 2.4: velocity profiles of Laminar flow and turbulent flow (<https://engineeringlibrary.org>).

When considering the viscous forces for a high Reynolds number, the inertia forces are greater. As a result, the arbitrary and quick variations in the fluid that cause the flow to become turbulent cannot be prevented by the viscous forces (Bergman T. L. 2011).

The imbalanced movement of the fluid's particles is what defines turbulent flow. There isn't any particular regularity, like in wave motion. There is no clear layering, and the fluid particles travel in random directions with no discernible structure.

2.2.6 Flow in a Circular Tube

In practice for circular and noncircular pipes fluid flow is usually encountered. Blood flows over the bodies throughout by arteries and veins. By large pipelines oil and natural gas are transported. In our homes water that we use is drive through pipes. By wide piping networks water is distributed in the city. In a hydraulic space heating system, thermal energy is transmitted by the flow of water in the boiler, and then it is distributed to the preferred spot through pipes.

2.3 Heat Transfer



Figure 2.5: Heat transfer in a solid (<https://www.snexplores.org>).

2.3.1 What is Heat Transfer?

Heat transfer is a transmit process of energy due to temperature difference. In a medium or between media if there is a temperature difference then heat transfer must take place. Heat can be transferred by conduction, convection or radiation.

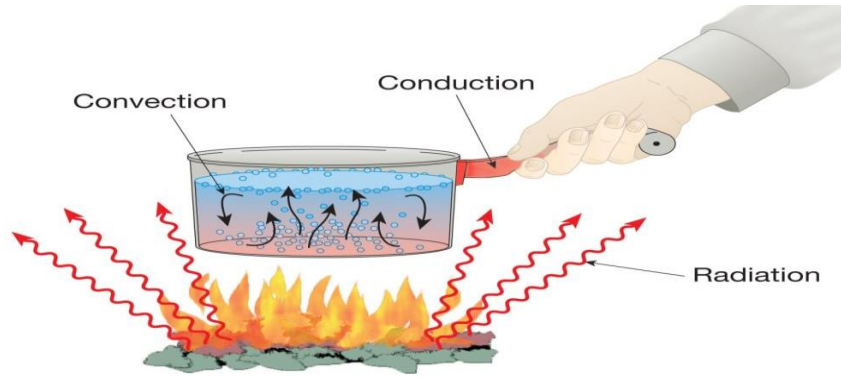


Figure 2.6: Heat Conduction, Convection and Radiation (<https://www.simscale.com>).

Conduction: In a stationary medium, if a temperature gradient exists and the heat transfer happens across the medium then this kind of heat transfer is called conduction.

Convection: In convection, heat is transferred when there is a temperature differential between a moving fluid and a surface.

Radiation: Heat transfer by radiation in the absence of a superseding medium between two surfaces at different temperatures. In this kind of heat transfer whole the surfaces of finite temperature release energy by electromagnetic waves.

2.3.2 Hydraulic Diameter (D)

Hydraulic diameter can be expressed as the ratio of four times the cross sectional area to the wetted perimeter of the channel. For plain tube, hydraulic diameter (D_h) can be written as,

$$D_h = \frac{4\pi D_i^2 / 4}{\pi D_i}$$

$$D_h = D_i.$$

Where, D_i notes tube's inside diameter.

For circular pipes the diameter of the pipe is taken as the hydraulic diameter.

2.3.3 Average Wall Temperature (T_w)

Average wall or surface temperature of the fluid is calculated by using thermocouple at different points in experimental session. Whenever in our simulation, we count it

from average temperature for all the point on the surface of the fluid domain. Fluid surface is very close to heat exchanger surface so the surface temperature is too high compare to the bulk temperature.

2.3.4 Bulk Temperature / Average Fluid Temperature (T_b)

The mean or bulk temperature of the fluid is defined as the thermal energy transported by the fluid particles when it moves. The rate of transportation may be attained by integrating the product of the mass flux (ρu) and the internal energy per unit mass ($C_p T$) for the fluid domain. The bulk temperature represents the total energy of the flow at any exacting location. Average fluid temperature is calculated by taking the average of inlet and outlet temperature and it expresses as:

$$T_b = \frac{T_{out} + T_{in}}{2}.$$

Where, T_{in} and T_{out} are the inlet and the outlet average temperature.

2.3.5 Thermal Conductivity (k)

The Thermal conductivity is a measure of how quickly thermal energy diffuses across a substance. This process is represented by the Fourier's law of heat conduction, which is usually expressed as follows:

$$q = -k \frac{dT}{dy},$$

where the temperature gradient component in the y direction is represented by the symbol dT/dy , which is chosen to agree with the velocity gradient component emerging in Newton's law of viscosity, and k indicates the thermal conductivity. The heat flux q is defined as the amount of heat per unit area at a given time. When it comes to fluids, particularly gases, their behavior is comparable to that of μ in terms of temperature fluctuations, even if the underlying physics for both attributes is the same.

2.3.6 Heat Transfer rate (Q)

The Heat transfer is the process of transferring thermal energy between two bodies or among the bodies which have a temperature difference. Transferring of heat takes place in such a way that until the surroundings or the body reaches in thermal equilibrium. We call the quantity of energy transmitted per unit of time the heat transfer rate. The heated tube's surface will transfer heat to the low-temperature fluid as it flows through it.

Then the heat transfer rate (Q) to the fluid is defined as follows:

$$Q = mC_p(T_{out} - T_{in}).$$

Where, the inlet temperature of the cold fluid is T_{in} , T_{out} is the outlet temperature of the bulk fluid and m is the mass flow rate.

For tube, with perforated rectangular strip inserts, heat transfer rate at per unite area of the fluid will be

$$q = \frac{Q}{A}.$$

In our simulation, we applied the thermal boundary conditions for a constant heat flux.

2.3.7 Heat Transfer Coefficient (h)

The amount of heat conveyed for a unit temperature difference between the fluid or fluids and unit area of surface in unit time is called the heat transfer coefficient (h). The value of ' h ' depends on many factors of fluid properties, such as thermodynamic, transport properties of fluid flow, fluid flow nature, geometry of the surface and existing thermal conditions. At the similar flow field, the heat transfer coefficient is higher for turbulent flow, than the laminar flow. In a tube with perforated rectangular strip inserts the heat transfer coefficient (h) represents a significant effect instead of a plain tube. The heat transfer coefficient for the tube with perforated rectangular strip inserts and the plain tube can be expressed as follows:

$$h = \frac{q}{T_w - T_b}.$$

Where, q is the heat flux, T_w represent the wall temperature and T_b denote the bulk fluid temperature.

2.3.8 Nussalt Number (Nu)

To analyze the heat transfer characteristics of a flow the Nusselt number plays a vital role. The augmentation of heat transfer from a surface that arises in a real-world scenario is calculated using this dimensionless quantity, as opposed to the heat transmitted if only conduction occurred. The enhancement of heat transfer by convection is implied by the increasing of the value of the Nusselt number. The Nusselt number is equal to the dimensionless temperature gradient at the surface. The definition of the Nusselt number is:

$$Nu = \frac{hD}{k},$$

where D represents the tube's diameter and k denotes the fluid's heat conductivity. The Nusselt number is considered to be the dimensionless convection heat transfer coefficient and is named for Wilhelm Nusselt, who made important contributions to convective heat transfer in the first half of the 20th century. The Nusselt number is a measure of the increase in heat transmission through a fluid due to convection as opposed to conduction across the same fluid layer.

2.3.9 Pressure Drop (ΔP)

A pressure drop caused by viscous effects is an example of an irreversible pressure loss; this is known as pressure loss. The pressure drop would be zero in the absence of friction, as it is proportionate to the fluid's viscosity. At the time of passing fluid through a tube, due to the frictional forces pressure drop will occur in the tube. Pressure drop is the hydraulic loss caused by the surface over in which the fluid is moving. Pressure drop is used to describe the decrease in pressure from one point to another point in the downstream of a pipe or a tube. Increased blower power is required for fluid to flow over the surface when there is a greater pressure drop. The drop of pressure is high for rough surface. One can compute the friction factor by utilizing the pressure drop.

Pressure drop is given by the following equation

$$\Delta P = P_i - P_o.$$

Where,

ΔP = Pressure drop (N/m^2)

P_i = Pressure at inlet (N/m^2)

P_o = Pressure at outlet (N/m^2)

2.3.10 Friction Factor (f)

The friction factor has been resolute to depend on the Reynolds number for the flow and the degree of roughness of the pipe's inner surface. In the chemical and process industries friction factor is used to determine the friction characteristics.

The friction factor is given by,

$$f = \frac{\Delta p}{\left(\frac{L}{D}\right) \left(\frac{\rho v^2}{2}\right)} .$$

Where,

f = friction factor

ρ = Density of fluid (kg/m^3)

v = Velocity of fluid in the tube (m/s)

D = Inside diameter of the tube (m)

L = Length of the tube (m)

2.4 Heat Exchanger

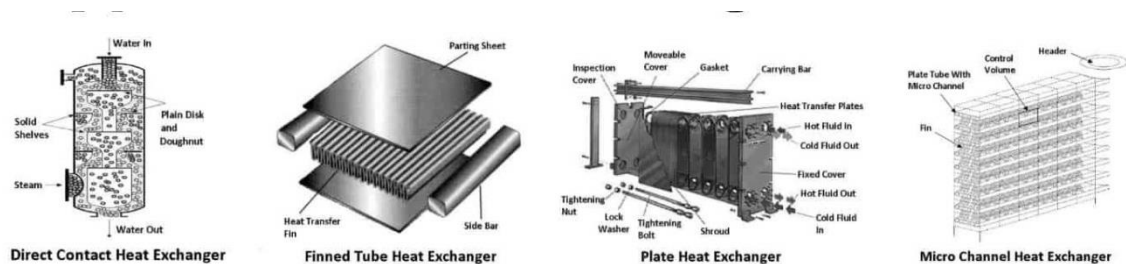


Figure 2.7: Types of heat exchanger (<https://www.theengineerspost.com>).

2.4.1 What is Heat Exchanger?

Transferring thermal energy between two or more fluids, between a solid surface and a fluid, or between two solid surfaces and a fluid at different temperatures and in

thermal contact is accomplished with the use of heat exchanger equipment. There are generally no external heat and work exchanges in heat exchangers. Classic applications involve heating or cooling of a fluid and evaporation or condensation of single or multi component fluid.

2.4.2 Classification of Heat Exchangers

Heat exchangers have extensive industrial and domestic applications. The applicable design of heat exchangers is a very complicated problem. It involves many other things than the heat-transfer analysis alone. Installation, weight, size and production cost play important roles in the selection of the final design of a heat exchanger. In many cases, even though cost is an important consideration, size and footprint often tend to be the main factors in choosing a design.

The fluids exchanging heat are in direct contact in a few heat exchangers. In most heat exchanger device, enhancement of heat between fluids comes to pass through a separating wall or into and out of a wall in a temporary conduct. In many heat exchangers, a heat transfer surface separated the fluids and preferably the fluids do not mix. Such kind of exchanger is mentioned as direct transfer type. In the other hand,

The exchangers in which exchange heat between the hot and cold fluids—via thermal energy storage and discharge through the exchanger exterior or matrix— are known as indirect transfer type. A classification chart of heat exchanger is given below:

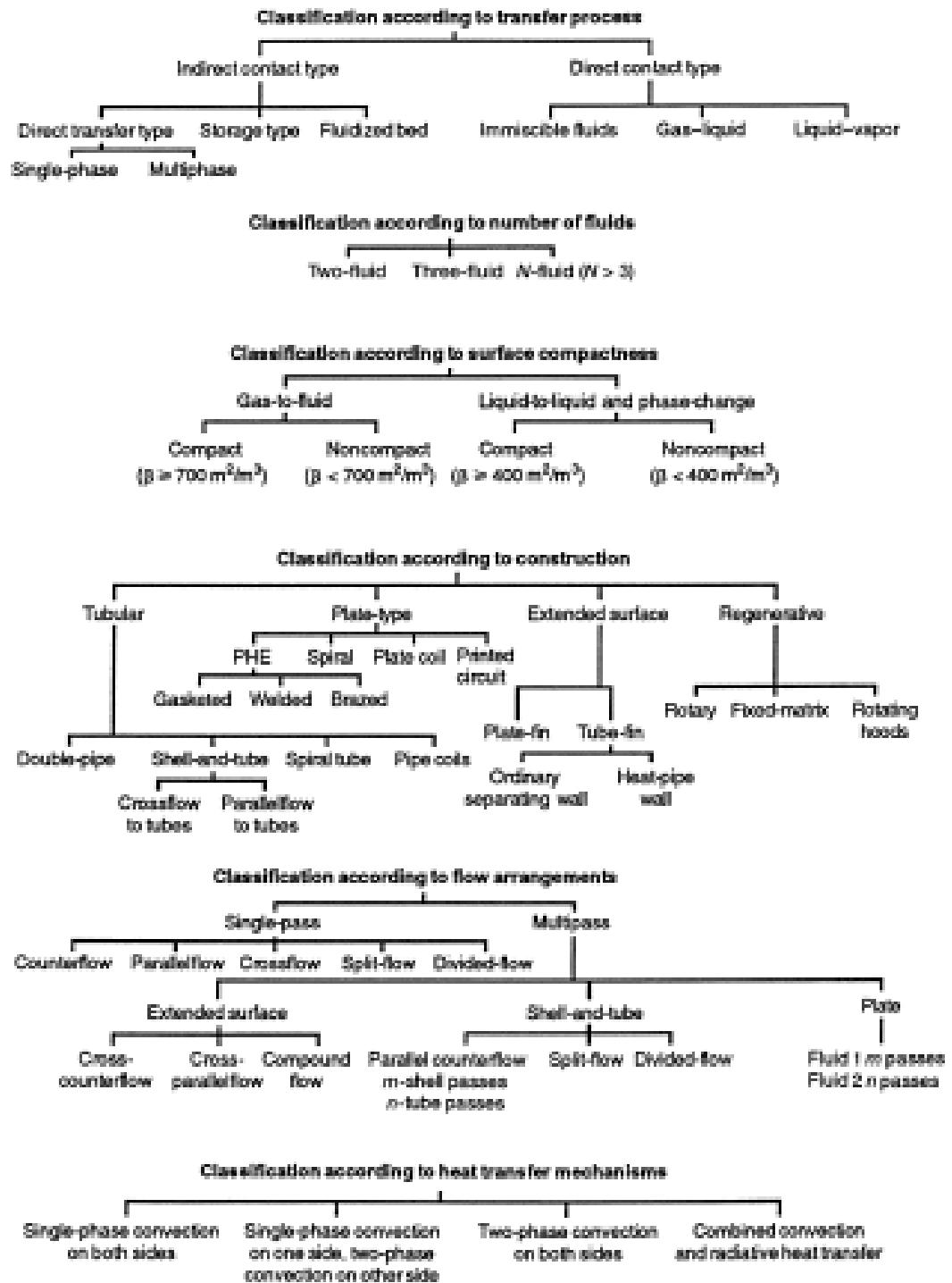


Figure2.8: Classification of heat exchangers (Kakaç, S.1981)

2.4.3 Porosities (R_p)

The empty spaces in a material are measure by Porosity. It is measured as a percentage between 0 -100% or as a fraction between 0-1. It varies with pore diameter and distance between two pore. It increases with the raises of pores diameter or with reduce of central distance between the two neighboring pores. Higher porosity

influence higher flow rate of fluid and lower porosity manipulate lower flow rate of fluid ([Bhuiya M.M.K. 2008](#)).

Porosity of the strip inserts can be defined as follows,

$$R_p = \frac{\text{Total pores area}}{\text{Total insert area}}$$

$$R_p = \frac{\frac{\pi}{4} d^2}{L \times W}.$$

Where,

d = Pore diameter (mm)

L = Length of the insert (m)

W = Width of the insert (m)

2.5 Computational Methods

Differential equations are used in the science and engineering fields to administer the majority of practical situations. It is rare to find perfect solutions to governing equations because of loads and geometrical constraints. Therefore, approximation techniques for differential equation solving are crucial for issue analysis in numerous fields.

2.5.1 Finite difference Method

Finite difference method (FDM) is established at the application of a local Taylor expansion to approximate the differential equations. The FDM uses a topologically square network of lines to construct the discretization of the PDE. This method is used to handle complex geometries in multiple dimensions. This topic irritated the use of an integral form of the PDEs and then the development of the finite element and finite volume techniques ([Peiro, J. et al. 2005](#)).

2.5.2 Finite Volume Method

A discretization technique for partial differential equations, particularly those arising from physical conservation rules, is the finite volume method (FVM). Using structured or unstructured meshes, FVM may be applied to any geometry and produces intensive systems. The local conservativeness of the numerical fluxes, or the

numerical flux's conservation from one discretization cell to its neighbor, is an additional property. When modeling issues where flux is important, like in fluid mechanics, semi-conductor device simulation, heat, and mass transport, the finite volume method becomes highly appealing due to this final property. Because it relies on a "balance" approach, the finite volume method is locally conservative. A local balance is written on each discretization cell, also known as the "control volume," and an integral formulation of the fluxes over the control volume's boundary is subsequently obtained using the divergence formula. It discretizes the fluxes on the boundary with regard to the discrete unknowns ([Chen L.](#)).

2.5.3 Boundary Element Method

Conventionally, boundary integral equations are used to analyze boundary value problems for partial differential equations. Any approach for the approximate numerical solution of these boundary integral equations is referred to as the "boundary element method" (BEM) ([Ciarlet, P. G. 1990](#)). Being an exact solution of the differential equation in the domain and parameterized by a finite set of parameters existing on the boundary, the approximate solution of the boundary value problem obtained by BEM has one unique property.

2.5.4 Finite Element Method

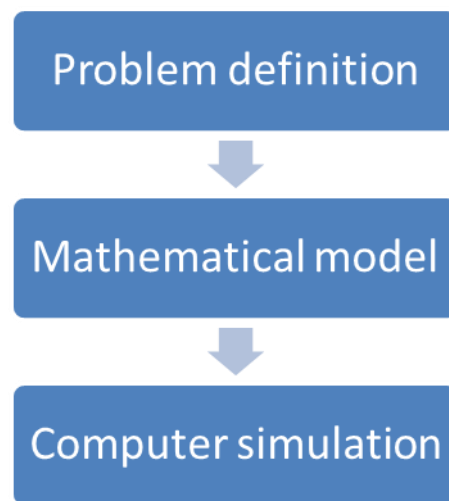
The finite element method (FEM) is a computational method to find the approximate solutions to boundary value problems for PDE. It is also known as finite element analysis (FEA). It used on subsection of a whole domain into smaller parts, called finite elements, and variation method from the calculus for solving the problem by minimizing a related error function. FEM integrate methods for involving many simple element equations over many small sub-domains, named finite elements, to approximate a more complex equation over a larger domain ([Yu, W. H.et al. 2006](#))

2.6 Computational Fluid Dynamics

Fluid flows are governed by the Partial Differential Equations (PDE) that present conservation laws for mass, momentum and energy. The Computational Fluid Dynamics (CFD) is the skill to replace those PDE systems by a set of algebraic

equations which can be solved using computers. CFD runs a qualitative calculation of fluid flows all the way through mathematical modeling, numerical methods and software tools. Until now, CFD was mostly functional to single phase flow and complexities occurred when dealing with two different phase laminar and turbulent flow owing to high computational requirement.

There are three important steps in the computational modeling of any physical process:



2.7 Previous Studies

The exchange of heat between fluid to fluid or fluids and solid to fluid depend on the characteristics of fluid, fluid flow activities and heat exchanger performance. In industrial and engineering applications, an efficient heat transfer device plays an important role. So it's an essential need by researchers to improve the overall performance of heat exchanger device. A high performance and cost effective heat exchanger design is most complicated. Early of the twentieth century many researcher studied about this. The performance of heat exchanger may improve by using many techniques such as rough surface, inserts etc.

For laminar flow [Saha S. K. et al\(1989\)](#) examined the heat transfer and pressure drop phenomenon with twisted tape inserts fitted tube and state that the standard spaced twisted tape inserts exposed perform significantly than the full length twisted tape inserts. [Date A. W.](#) and [Gaintonde U. N. \(1990\)](#) developed correlations for the laminar flow in a pipe using regular spaced twisted tape inserts and predicting characteristics for the flow dynamics.

[Peng Lie et al. \(2018\)](#) observed that the Nusselt number and friction factor are proportional to the number of conical strips and central angle and reciprocal to the pitch in an experimental and numerical examination with multiple conical strip insertion tubes.

The Nusselt number and friction factor gives 2.54 – 7.63 and 2.40 – 28.74 times higher than the plain tube. They also added the increasing of slant angle primarily enhance and then reduce the Nusselt number and friction factor. [Tam L. M. and Ghajar A. J. \(2006\)](#) investigate the transitional heat transfer with different inlet configuration fitted plain horizontal pipes and presented a flow regime map for the forced convection and mixed convention transitional flow. This map helps the researcher to determine the influence of bounciness. For the transitional flow [Meyer J. P. and Abolarin S. M. \(2018\)](#) study with a square-edge inlet and twisted tape inserts fitted circular tube and notified that Colburn j-factor increases inversely with twisted ratios.

For the constant twist ratios heat flux also varies and the transition begins laminar to transitional flow overdue by higher heat flux. At the constant twisted ratio and the Reynolds number friction factor and heat flux remain changed inversely. [Pengxiao Li](#)

et al(2017) investigated numerical and experimental proceedings at drainage inserts in a pipe and proposed that the slant angle 45° is the best slant angle for the inserts and the PEC range recognized 0.95 to 1.04 at the pitch ratio of 3.3. In a review of square duct fitted circular tube with swirl flow generator Patil S.V. and Vijay Babu P.V. (2011) suggested a twisted tape inserts gives better performance in laminar flow than in turbulent flow and the heat transfer of circular tube is lower than of square ducts. In further addition was that the short-length and regular spaced twisted tapes achieve considerable better than the full-length twisted tapes. An experimental and numerical comparison of the wave fin and the louvered fin with round tube heat exchanger were investigated by Okbaz A. K. *et al*(2018) and they established that the Colburn factor j , Fanning friction factor f and JF factor of the louvered fin heat exchanger exposed notable performance compare to the wave fin with round tube heat exchanger. In a different presentation of the louvered strip insert, Indri Yaningsih and Agung Tri Wijayanta (2017) recommended that the minimum pitch length give the maximum Nusselt number, friction factor, and heat transfer coefficient ratio. They noted that the average heat transfer increases up to 67%–77%, 48%–53%, and 21%–24% compared to plain tube for pitch lengths of 40, 50, and 60 mm, respectively.

In a review study of Liu S. and Sakr M. (2013) suggested that the twisted tape inserts approved better in laminar flow instead of turbulent flow and also noted that the helical screw tape gives higher heat transfer rate then twisted tape inserts. They farther added the ribs, conical nozzle and conical ring perform more professional for turbulent flow. At the further analysis of Tabatabaeikia S. *et al*(2014) recommended for the louvered strip insert that the backward flow gives better performance than the forward one and also added that the jagged twisted tape insert influence finer Nusselt Number and thermal-hydraulic performance contrast with other twisted tape inserts, such as: classic twisted tape, butterfly insert, notched twisted tape and perforated twisted tape.

The heat transfer investigation of Delta-Winglet Twisted (DWT) tape inserts in a pipe Oblique Delta-Winglet Twisted (O-DWT) provide an enhanced efficiency then Straight Delta-Winglet Twisted (S-DWT) inserts was prescribed by Eimasa-ard S. *et al*.(2010) . At the rectangular cut twisted insert fitted tube Bodius Salam *et al*.(2013)

examine the outcome of Nusselt number and suggested that the heat transfer rate varies with Reynolds number. In a numerical examination of the rectangular box inserts tube [Sabbir Hossan et al.\(2015\)](#) added that the heat transfer rate is increases with the increasing of the distance among the inserts. [Bhuyan M. M. et al\(2017\)](#) also denote the equivalent result for U-loop circular pipe. [Suvanjan et al. \(2014\)](#) investigated various geometric parameters using computational fluid dynamics (CFD) in order to examine the flow characteristics of a laminar flow with a full-length twisted tape insert. An analytical numerical report on heat transfer for laminar flow using a V-cut twisted tape insert tube [Sami D. Salman et al. \(2013\)](#) advised that the V-cut twisted tape insert provides 107% heat enhancement with a reduced friction factor compared to the normal twisted tape inserts and other V-cut twisted tape inserts for twist ratio ($y = 2.93$) and cut depth ($w = 0.5$ cm). According to [Bhuyan M. M. et al. \(2017\)](#), who examined several twisted-type inserts statistically, full-length twisted inserts enhanced heat more than short-length twisted inserts.

The study of [Sadashiv and Madhukeshwara \(2014\)](#) recommended that whole-length helical tape with a centered rod enhance 160% and without a rod enhance 150% compared to plain tube for the numerical simulation of helical tape swirl generators with and without rods. According to [Matani A.G. and Rafik Md. Choudhari S. \(2015\)](#), who investigated triangle wave tape inserts, TWT-D3 type inserts outperform TWT-D1 and TWT-D2 type inserts in terms of Nusselt number, friction factor, and heat transfer coefficient. [Amol P. Yadav et al.\(2014\)](#) suggested inserts with an R_p of 4.5% for perforated twisted tapes, which boosted heat transfer performance more than inserts with lower porosities. This recommendation was made after reviewing the effects of various geometries on heat transfer performance. [Eiamsa-ard S. et al\(2010\)](#) suggested for the tube with twisted tape inserts and non-uniform wire coil that the twisted tape inserts with $y=3$ and DI-coil enhanced supreme thermal performance of 6.3% than the wire coil, 13.7% than the twisted tape inserts, 2.4% than the twisted tape inserts with uniform wire coil and 3.7% than the twisted tape inserts with D-coil. An experimental study conducted by [Chowdhuri M. A. K. et al\(2011\)](#) with rod-pin inserts tube and noted the rod-pin insert perform the best at the pin distance of 150mm and it about 9.8 times better than the plain tube. In a circular tube fitted with louvered strip inserts [Fan A.W. et al\(2012\)](#) reported that the louvered strip inserts augmented 4 times better Nusselt number than plain tube and the louvered inserts gives high

thermal performance for the slant angle ($\alpha = 20^\circ$) and pitch ($S = 30\text{mm}$) on the numerical simulation and found that it is easy to fabricate and can be widely used in the heat transfer exchanger technology .

An investigation of heat transmission in perforated disc baffles According to [El-Shamy A. R. \(2006\)](#), for perforated disc-baffles with an open area ratio of 18%, $S/De = 2$, and a Reynolds number of 48,024, the Nusselt number and friction factor increase by approximately three and six times, respectively, compared to plain tubes. Research by [Ta-Sung Huang et al.\(2008\)](#) on various types of insert tubes revealed that heat was improved more by flat plane inserts with holes than by twisted tape inserts with twist angles of 15.4° and 24.3° , respectively.

A thermal performance evaluation of Zigzag-Winglet perforated-tape (ZW-PT) inserts pipe [Suwannapan S. et al\(2015\)](#) enlisted that the Re is proportional with Nu and reciprocal with the f and also added the 45° ZW-PT inserts with pitch ratio ($PR=1.0$) and the blockage ratio ($BR=0.15$) augment the superior thermal efficiency factor (TEF) for the lowest Reynolds number.

[Ahamed J. U. et al.\(2007\)](#) and [Ahamed J. U. et al.\(2011\)](#) experimentally examined with the perforated twisted inserts tube and locate that the porosities(R_p) of 4.6% enhance supreme amount of heat then the other porosities for the perforated twisted inserts tube.

In the same experiment, $R_p = 4.5\%$ was found to provide a better presentation than other methods by [Bhuiya M. M. K. et al.\(2013\)](#). According to [Mizanuzzaman et al.\(2013\)](#), the porosities of 15.85% for the X-shaped longitudinal perforated insert tube provide greater efficiency than the other porosities for the same inserts. According to [Bhuiya M. M. K. et al.\(2012\)](#) experimental investigation of perforated rectangular strip insert tubes, the tube with 4.4% porosity boosted the maximum heat transfer coefficient, reaching a value that was up to 2.3 times more than that of a plain tube. A numerical study for the axial perforated inserts fitted U-loop circular tube [Acherjee S. et. al.\(2016\)](#) noted that for the laminar flow the porosity of 4.42% enhanced the highest amount of heat.

From the above literature it is clear that the perforated type inserts plays better perform than the plain tube and plain type inserts. But no literatures are found with the effect of angle of perforation. Thus reason interrogate us to run this investigation

and we assume that this type of investigation helps us to understand better performance of heat transfer analysis.

For the simulation we choose a non-isothermal laminar flow for the physics and water as an acting fluid. The simulation is performed to examine the influence of angle of perforation on heat transfer rate and fluid flow characteristic. We compared the results with perforated inserts tube and plane tube. This examine lead us to calculate the effect of angle on performance and evaluate the heat transfer augmentation and the pressure drop.

Chapter 3

Mathematical Model and Computational Domain

3.1 Conservation of Fluid and Heat Transfer Equations

A series of equations based on fundamental conservation laws must be the first step in solving a novel problem involving momentum, heat, and mass transfer in a fluid using physical systems. These formulas include:

1. The equation for continuity (mass conservation).
2. The motion equation, which accounts for momentum conservation.
3. The energy equation, also known as the first law of thermodynamics or the conservation of energy.
4. The formula for species conservation (conservation of species).

According to time and position within the system, these equations depict changes in concentration, temperature, and velocity. For issues pertaining to a pure fluid, the initial three equations suffice. For a combination of chemical species, the fourth equation is required.

3.1.1 The Control Volume

A control volume must be chosen at the time of calculating the conservation equations. While, for simplicity's sake, the most appropriate shape is usually assumed, the derivation can be carried out for a volume element of any shape in a given coordinate system. In Figure 3.1, various coordinate systems are displayed. When selecting a control volume, we can use a volume that is fixed in space and allows the fluid to flow through the boundaries, or we can use a volume that is fixed with a fixed mass of fluid and moves with the fluid. The Eulerian viewpoint is the first, while the Lagrangian viewpoint is the second. The outcomes are the same for both strategies.

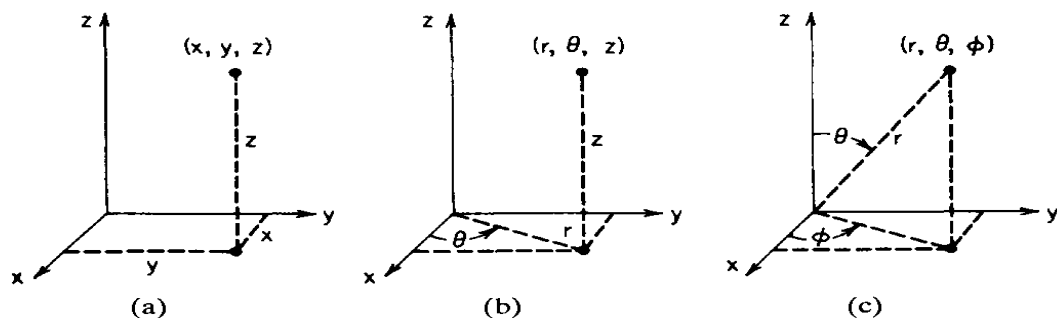


Figure 3.1: Coordinate systems (a) Rectangular, (b) Cylindrical, (c) Spherical.

3.1.2 The Partial Time Derivative $\partial B/\partial t$

The way a continuum property, B , changes over time at a fixed point in space is indicated by the partial time derivative of $B(x, y, z, t)$. Otherwise, the change in B with t as noticed by a stationary observer is represented as $\partial B/\partial t$.

3.1.3 Total Time Derivative DB/Dt

Following is the relationship between the partial time derivative and the total time derivative:

$$\frac{dB}{dt} = \frac{\partial B}{\partial t} + \frac{dx}{dt} \frac{\partial B}{\partial x} + \frac{dy}{dt} \frac{\partial B}{\partial y} + \frac{dz}{dt} \frac{\partial B}{\partial z}, \quad (3.1)$$

where dx/dt , dy/dt and dz/dt represent the constituents of an observer's velocity in motion. The change in B over time as observed by the moving viewer is therefore represented by dB/dt .

3.1.4 Substantial time derivative DB/Dt

This derivative is a unique type of total time derivative in which the viewer's velocity is exactly the same as the flow's velocity, meaning they follow the current:

$$\frac{DB}{Dt} = \frac{\partial B}{\partial t} + u \frac{\partial B}{\partial x} + v \frac{\partial B}{\partial y} + w \frac{\partial B}{\partial z}, \quad (3.2)$$

where the constituents of the local fluid velocity \mathbf{V} are represented by the variables u , v , and w . One can alternatively identify the derivative subsequent to motion as the significant time derivative. Since it shows the change in B as a result of translation, the sum of the final three terms on the right side of Eq. (3.2) is referred to as the convective contribution.

The operator D/Dt is used to reorganize several conservation equations related to the volume element fixed in space to an element following the fluid motion.

The operator D/Dt may also be articulated in vector form:

$$\frac{D}{Dt} = \frac{\partial}{\partial t} + (\mathbf{V} \cdot \nabla). \quad (3.3)$$

3.2 Continuity Equation

Conservation of mass principle is one of the most essential physical laws of governing motion of any continuous medium. The derivation of the equation by application of this principle is recognized as continuity equation.

In a three-dimensional fluid flow, Figure 3.2 depicts a differential volume (control volume) positioned at a random, fixed place. The components of velocity \vec{u} , parallel to the x, y, and z axes in the Cartesian axis, are represented by the symbols u, v, and w, respectively.

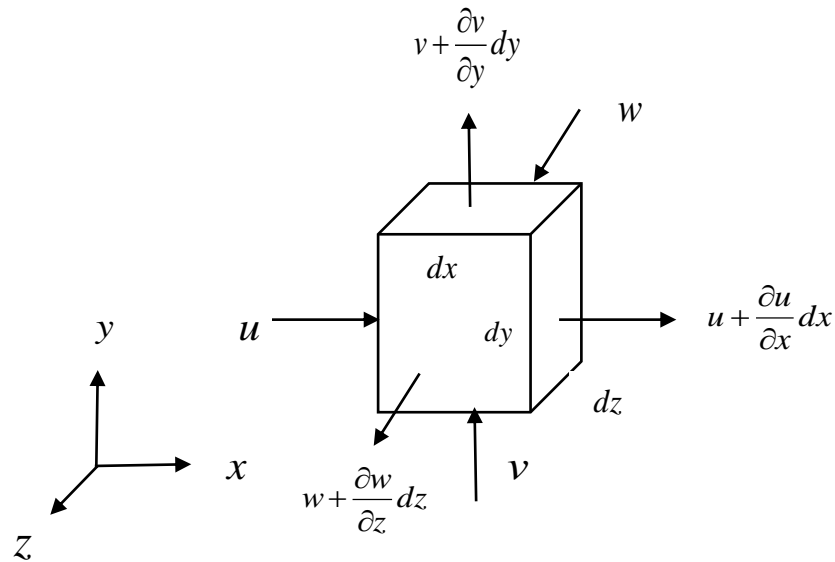


Figure 3.2: Differential volume element in three dimension.

Achieving equilibrium between the net mass flow rate into the volume and the temporal rate of mass change within it is required by the concept of conservation of mass. Total mass inside the volume is ρdV .

Since dV is constant, we have

$$\frac{\partial \rho}{\partial t} dV = \sum (\text{mass flow in} - \text{mass flow out}). \quad (3.4)$$

Here the partial derivative is applied since density may vary in space as well as time.

The rate of change of mass in the control volume from the flow in x-direction is

$$m'_x = \rho u dy dz - \left[\rho u + \frac{\partial(\rho u)}{\partial x} dx \right] dy dz \quad (3.5)$$

Likewise, the comparable words that result from the flow in the directions of y and z are

$$m'_y = \rho v dx dz - \left[\rho v + \frac{\partial(\rho v)}{\partial y} dy \right] dx dz \quad (3.6)$$

$$m'_z = \rho w dx dy - \left[\rho w + \frac{\partial(\rho w)}{\partial z} dz \right] dx dy \quad (3.7)$$

Thus, the rate at which mass changes becomes,

$$\frac{\partial \rho}{\partial t} = m'_x + m'_y + m'_z = - \left[\frac{\partial(\rho u)}{\partial x} + \frac{\partial(\rho v)}{\partial y} + \frac{\partial(\rho w)}{\partial z} \right] dx dy dz \quad (3.8)$$

Since $dV = dx dy dz$, the equation (3.4) can be written as

$$\frac{\partial \rho}{\partial t} + u \frac{\partial \rho}{\partial x} + v \frac{\partial \rho}{\partial y} + w \frac{\partial \rho}{\partial z} + \rho \left[\frac{\partial u}{\partial x} + \frac{\partial v}{\partial y} + \frac{\partial w}{\partial z} \right] = 0 \quad (3.9)$$

This equation is the continuity equation for a general three dimensional flow expressed in Cartesian co-ordinates (Hutton D. 2004). The continuity equation can also be written in other forms

$$\frac{\partial \rho}{\partial t} = -(\nabla \cdot \rho \mathbf{V}) \quad (3.10)$$

and

$$\frac{D\rho}{Dt} = -\rho(\nabla \cdot \mathbf{V}), \quad (3.11)$$

where the derivative $\frac{D\rho}{Dt}$ is the rate of change of density following a fluid particle.

For incompressible fluid the equation becomes

$$\nabla \cdot \mathbf{V} = 0. \quad (3.12)$$

3.3 Equation of motion

The momentum equation for a stationary volume element with gravity as the only body force is given by

$$\frac{\partial \rho \mathbf{V}}{\partial t} = -(\nabla \cdot \rho \mathbf{V}) \mathbf{V} - \nabla P + \nabla \cdot \boldsymbol{\tau} + \rho \mathbf{g}. \quad (3.13)$$

Where $\frac{\partial \rho \mathbf{V}}{\partial t}$ is the momentum increase rate per unit volume, $(\nabla \cdot \rho \mathbf{V}) \mathbf{V}$ indicates the rate of momentum gain by convection per unit volume, ∇P indicates the pressure force on the element per unit volume, $\nabla \cdot \boldsymbol{\tau}$ indicates the rate of momentum gain by viscous transfer per unit volume, and $\rho \mathbf{g}$ indicates the gravitational force on the element per unit volume. The equation of continuity can be used to reorganize equation (3.13), giving

$$\rho \frac{D\mathbf{V}}{Dt} = -\nabla P + \nabla \cdot \boldsymbol{\tau} + \rho \mathbf{g}. \quad (3.14)$$

Newton's second law of motion is announced in the last equation, which takes the form

$$\text{Mass} \times \text{Acceleration} = \text{sum of Forces}.$$

The equation of motion in its two forms (Eqs. 3.13 and 3.14) is equivalent to the equation of continuity in its two forms (Eqs. 3.10 and 3.11). It is mentioned that Eqs. 3.13 and 3.14 solely take into account gravity as a body force. Eq. 3.14 becomes the flow of a Newtonian fluid with variable density but constant viscosity.

$$\rho \frac{D\mathbf{V}}{Dt} = -\nabla P + \frac{1}{3} \mu \nabla (\nabla \cdot \mathbf{V}) + \mu \nabla^2 \mathbf{V} + \rho \mathbf{g} \quad (3.15)$$

If ρ and μ are constant, Eq. 3.15 may be simplified for the equation of continuity ($\nabla \cdot \mathbf{V} = 0$) for a Newtonian fluid to give

$$\rho \frac{D\mathbf{V}}{Dt} = -\nabla P + \mu \nabla^2 \mathbf{V} + \rho \mathbf{g} \quad (3.16)$$

This is the vector version of the well-known Navier-Stokes equation.

3.4 Energy Equation

For a stationary volume element through a pure fluid flow, the energy equation reads

$$\frac{\partial}{\partial t} \rho \left(\mathbf{u} + \frac{1}{2} V^2 \right) = -\nabla \cdot \rho \mathbf{V} \left(\mathbf{u} + \frac{1}{2} V^2 \right) - \nabla \cdot \mathbf{q}'' + \rho (\mathbf{V} \cdot \mathbf{g}) - \nabla \cdot P \mathbf{V} + \nabla \cdot (\boldsymbol{\tau} \cdot \mathbf{V}) + q'''. \quad (3.17)$$

The rates of energy gain per unit volume $\frac{\partial}{\partial t} \rho \left(\mathbf{u} + \frac{1}{2} V^2 \right)$, energy input per unit volume $-\nabla \cdot \rho \mathbf{V} \left(\mathbf{u} + \frac{1}{2} V^2 \right)$, energy input per unit volume $-\nabla \cdot \mathbf{q}''$, rate of work done on the fluid per unit volume by gravity forces $\rho (\mathbf{V} \cdot \mathbf{g})$, rate of work done on the fluid per unit volume by pressure forces $-\nabla \cdot P \mathbf{V}$, rate of work done on the fluid per unit volume by viscous forces $\nabla \cdot (\boldsymbol{\tau} \cdot \mathbf{V})$, and rate of heat generation per unit volume q''' are represented here. q''' is the source term.

where u denotes the energy within. The fluid's potential energy is integrated into the work component on the right side of the equation, which represents the rate of increase of internal and kinetic energy. Therefore, it is absent from the left side of the equation. With the use of the equations of continuity and motion, Eq. (3.17) may be rearranged to produce

$$\rho \frac{D\mathbf{u}}{Dt} = -\nabla \cdot \mathbf{q}'' - P(\nabla \cdot \mathbf{V}) + \nabla \mathbf{V} : \boldsymbol{\tau} + q''' \quad (3.18)$$

For a Newtonian fluid,

$$\nabla \mathbf{V} : \boldsymbol{\tau} = \mu \Phi. \quad (3.19)$$

Working in terms of enthalpy instead of internal energy is frequently more convenient. The mass conservation equation, Eq. (3.11), and the definition of enthalpy, $i = u + P/\rho$ can be used to rearrange Eq. (3.18) to create

$$\rho \frac{Di}{Dt} = \nabla \cdot k \nabla T + \frac{DP}{Dt} + \mu \Phi + q''' \quad (3.20)$$

The Thermal energy can be expressed more conveniently in terms of fluid temperature and heat capacity than in terms of internal energy or enthalpy for the majority of engineering applications. Generally speaking, for pure materials,

$$\frac{Di}{Dt} = \left(\frac{\partial i}{\partial P} \right)_T \frac{DP}{DT} + \left(\frac{\partial i}{\partial T} \right)_P \frac{DT}{Dt} = \frac{1}{\rho} (1 - \beta T) \frac{DP}{Dt} + C_p \frac{DT}{Dt}, \quad (3.21)$$

where $\beta = \frac{1}{\rho} \left(\frac{\partial \rho}{\partial T} \right)_P$ replacing this into Eq. (3.20) we have the following common relations:

$$\rho C_p \frac{DT}{Dt} = \nabla \cdot k \nabla T + \beta T \frac{DP}{Dt} + \mu \Phi + q'''. \quad (3.22)$$

For an ideal gas, $\beta = \frac{1}{T}$ and then

$$\rho C_p \frac{DT}{Dt} = \nabla \cdot k \nabla T + \frac{DP}{Dt} + \mu \Phi + q'''. \quad (3.23)$$

It is observed that C_p does not have to be constant. Equation (3.20) might have been directly used to get Equation (3.23) by pointing out that for an ideal gas, $di = C_p dT$, where C_p is constant, and thus

$$\frac{Di}{Dt} = C_p \frac{DT}{Dt}. \quad (3.24)$$

Equation (3.18) ($du = C dt$) is utilized for an incompressible fluid with specific heat $C = C_p = C_v$. This allows us to derive

$$\rho C \frac{DT}{Dt} = \nabla \cdot k \nabla T + \mu \Phi + q'''. \quad (3.25)$$

It is easy to express equations (3.18), (3.20), and (3.22) in terms of momentum and energy. The energy equation ($q''' = 0$ for simplicity) is provided by Eq. (3.25). When dealing with solid materials, the density is often taken to be constant, $\mathbf{V} = 0$ can be specified, and Eq. (3.25) becomes

$$\rho C \frac{DT}{Dt} = \nabla \cdot k \nabla T + q'''. \quad (3.26)$$

It is the starting point for the majority of heat conduction issues ([Rohsenow et.al. 1998](#)).

3.5 Governing Equations for Simulation

To describe the heat transfer characteristics for the different angle oriented perforated insert in a circular pipe a numerical model is being formed. A generalization of energy equation and flow equation is useful to compute the numerical model. These the following equations are needed to explain the heat transfer phenomena in our simulation.

$$\rho \frac{\partial \mathbf{u}}{\partial t} + \rho(\nabla \cdot \mathbf{u}) = 0. \quad (3.27)$$

The rate of change of density at a fixed point in the fluid is expressed by equation (3.27).

$$\rho \frac{\partial \mathbf{u}}{\partial t} = \nabla \cdot \left[-p\mathbf{I} + \mu(\nabla \mathbf{u} + (\nabla \mathbf{u})^T) - \frac{2}{3}\mu(\nabla \cdot \mathbf{u})\mathbf{I} \right] + \mathbf{F}. \quad (3.28)$$

Equation of momentum defines by equation (3.28) which interprets the rate of change of momentum at per unit volume of the fluid. The left hand side of this equation represents the convective acceleration of the fluid particle.

$$\rho C_p \frac{\partial T}{\partial t} + \rho C_p \mathbf{u} \nabla T = \nabla \cdot (k \nabla T) + Q + Q_{vh} + W_p. \quad (3.29)$$

The heat transfer phenomena of fluid for unsteady condition represents by equation (3.29).

$$\text{Re} = \frac{\rho u D}{\mu}. \quad (3.30)$$

Equation (3.30) denotes the Reynolds number which expresses the ratio of the inertial force and the viscosity.

$$R_p = \frac{\frac{\pi}{4} d^2}{L \times W}. \quad (3.31)$$

Where L is the length, W is the width of the insert and “d” is the diameter of the pore. The heat transfer coefficient (h) was evaluated by

$$h = \frac{Q}{T_w - T_b}. \quad (3.32)$$

$$q = \frac{Q}{A}. \quad (3.33)$$

Where q is the constant heat flux, A is the surface area of the tube, T_w is the average wall temperature and T_b is the bulk temperature of the fluid flow.

$$T_b = \frac{T_{out} + T_{in}}{2}. \quad (3.34)$$

Where T_{in} and T_{out} are the inlet and outlet average temperature. The Nusselt number (Nu) is calculated by

$$Nu = \frac{hD}{k}. \quad (3.35)$$

Where D is the inside diameter of the tube and k is the thermal conductivity of water at the initial temperature. Then the friction factor (f) and thermal performance factor (η) expressed as follows:

$$f = \frac{\Delta p}{\left(\frac{L}{D}\right) \left(\frac{\rho v^2}{2}\right)}, \quad (3.36)$$

$$\eta = \frac{Nu}{Nu_o} \frac{1}{\left(\frac{f}{f_o}\right)^{\frac{1}{6}}}, \quad (3.37)$$

where η is the ratio between the heat transfer coefficient ratio and the friction factor ratio. Where Nu_o and f_o are the Nusselt number and friction factor for the 0° angle oriented tube.

3.6 Boundary Conditions

The diverse solution of the governing equations lies on the variety of compulsory boundary conditions.

The kinematic boundary conditions state the boundary kinematics for instance position, velocity. On a solid boundary, velocity of the fluid is equivalent to the velocity of the body.

$$\vec{u} = \vec{v} . \quad (3.38)$$

Where \vec{u} is the velocity of fluid and \vec{v} is the body surface velocity.

Tangential velocity component is the same as that of the rigid surface, which is known as no-slip condition (Yu, W. H. et al. 2006).

$$\vec{u} \cdot \hat{t} = \vec{v} \cdot \hat{t} . \quad (3.39)$$

The no-slip condition for viscous fluid states that at a solid boundary, the fluid will have zero velocity relative to the boundary.

$$\vec{u} = 0 , \quad (3.40)$$

while $u = u_o$ represents the inlet velocity in the velocity field for 0.014 ms^{-1} and 0.021 ms^{-1} an initial temperature $T = T_o = 293.15 \text{ K}$.

The outlet with zero normal stress is generated by the following equation.

$$\left[-p\mathbf{I} + \mu(\nabla\mathbf{u} + (\nabla\mathbf{u})^T) - \frac{2}{3}\mu(\nabla\mathbf{u})\mathbf{I} \right] \mathbf{n} = -f_0\mathbf{n} . \quad (3.41)$$

The amount of heat flux 32087 W/m^2 is taken as constant in our simulation.

3.7 Computational domain

The computational domain with the dimension of $3435.62\text{mm} \times 70\text{mm} \times 5\text{mm}$ in a tubular copper pipe is taken for our simulation. The dimension of rectangular copper inserts both are $1600\text{mm} \times 70\text{mm} \times 2\text{mm}$ fitted perpendicular with the fluid flow inside the tube. Where 20mm is the axial distance and 16mm is the transverse distance between two adjacent pores.

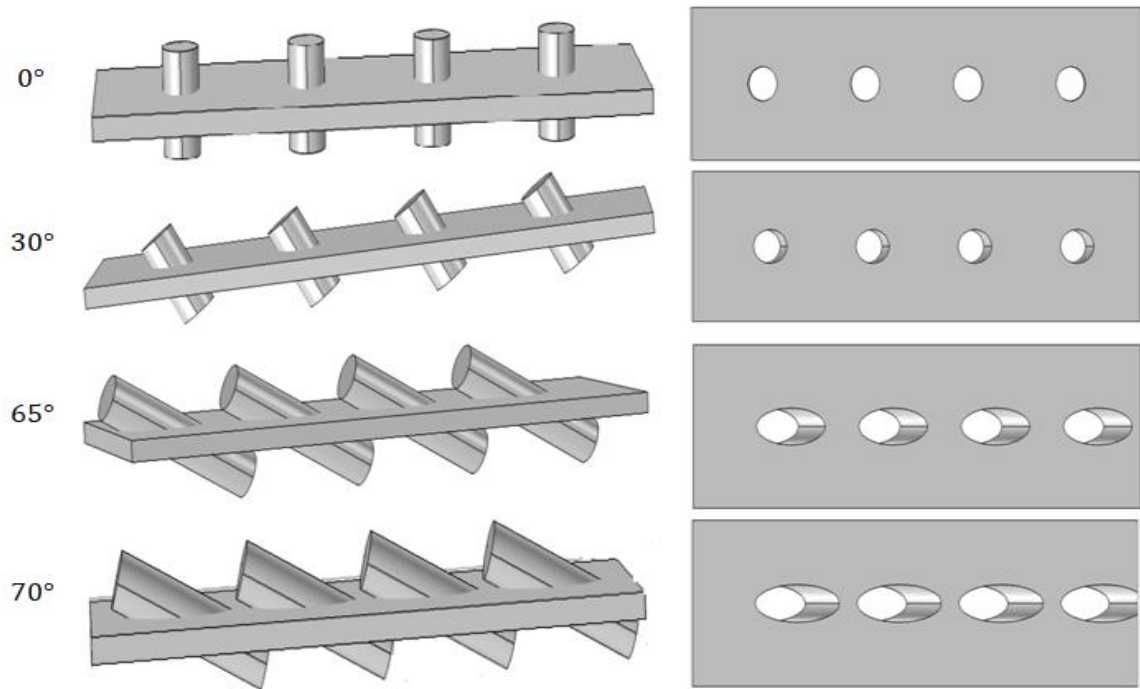


Figure 3.3: The angle orientation of rectangular strips inserts of the perforation angle of 0° , 30° , 65° and 70° .

The Figure 3.3 represents the angle orientation of rectangular strips inserts of the perforation angle of 0° , 30° , 65° and 70° used in the pipe and shows how it is taken. 0° is measured from perpendicular with the insert and then other angle were counted downward from this line.

The angle of perforation 0° , 5° , 10° , 15° , 16° , 17° , 20° , 30° , 40° , 50° , 60° , 65° , 68° and 70° respectively for the porosities of $R_p = 4.5\%$ represents in Figure 3.4. The computational domain of angle oriented perforated inserts U-loop pipe represents in Figure 3.5.

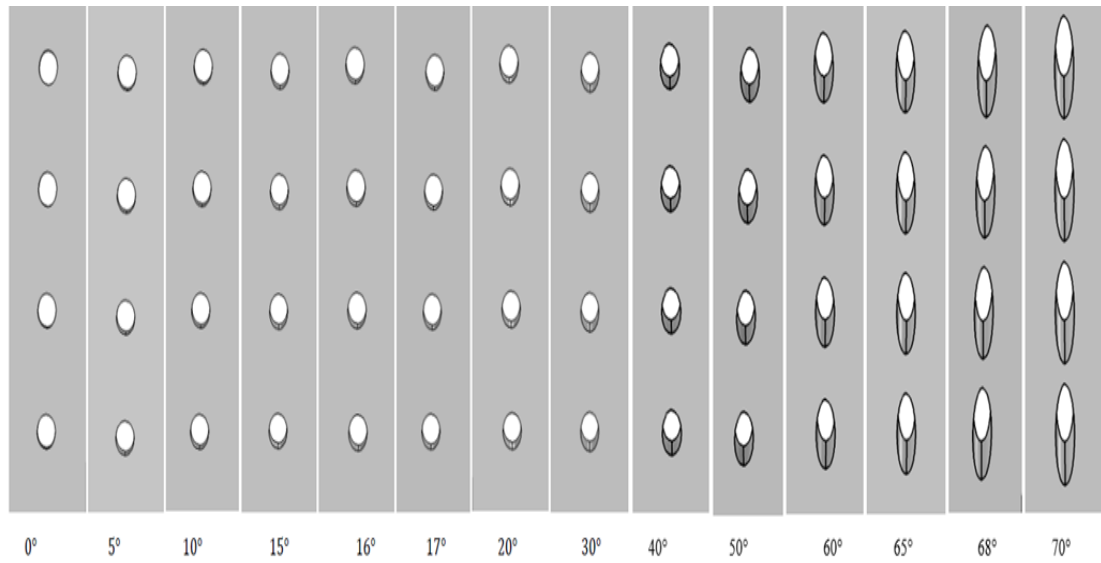


Figure 3.4: The angles of perforation $0^\circ, 5^\circ, 10^\circ, 15^\circ, 16^\circ, 17^\circ, 20^\circ, 30^\circ, 40^\circ, 50^\circ, 60^\circ, 65^\circ, 68^\circ$ and 70° respectively.

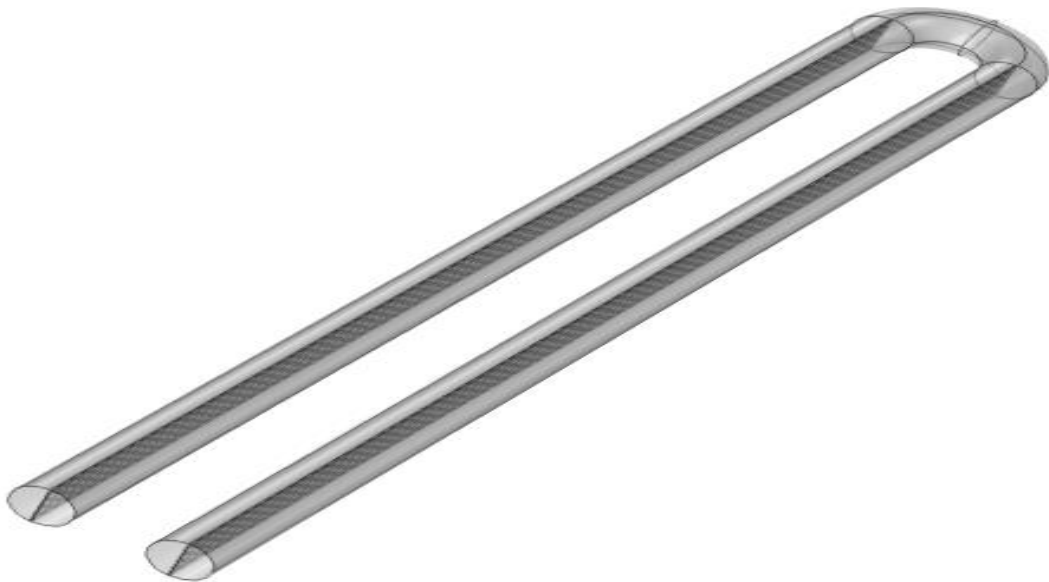


Figure 3.5: The computational domain of angle oriented perforated inserts U-loop pipe.

3.8 Mesh generation

In accuracy of computational results, the mesh design plays an important role. So we considered suitable mesh design for our simulation to achieve better results.

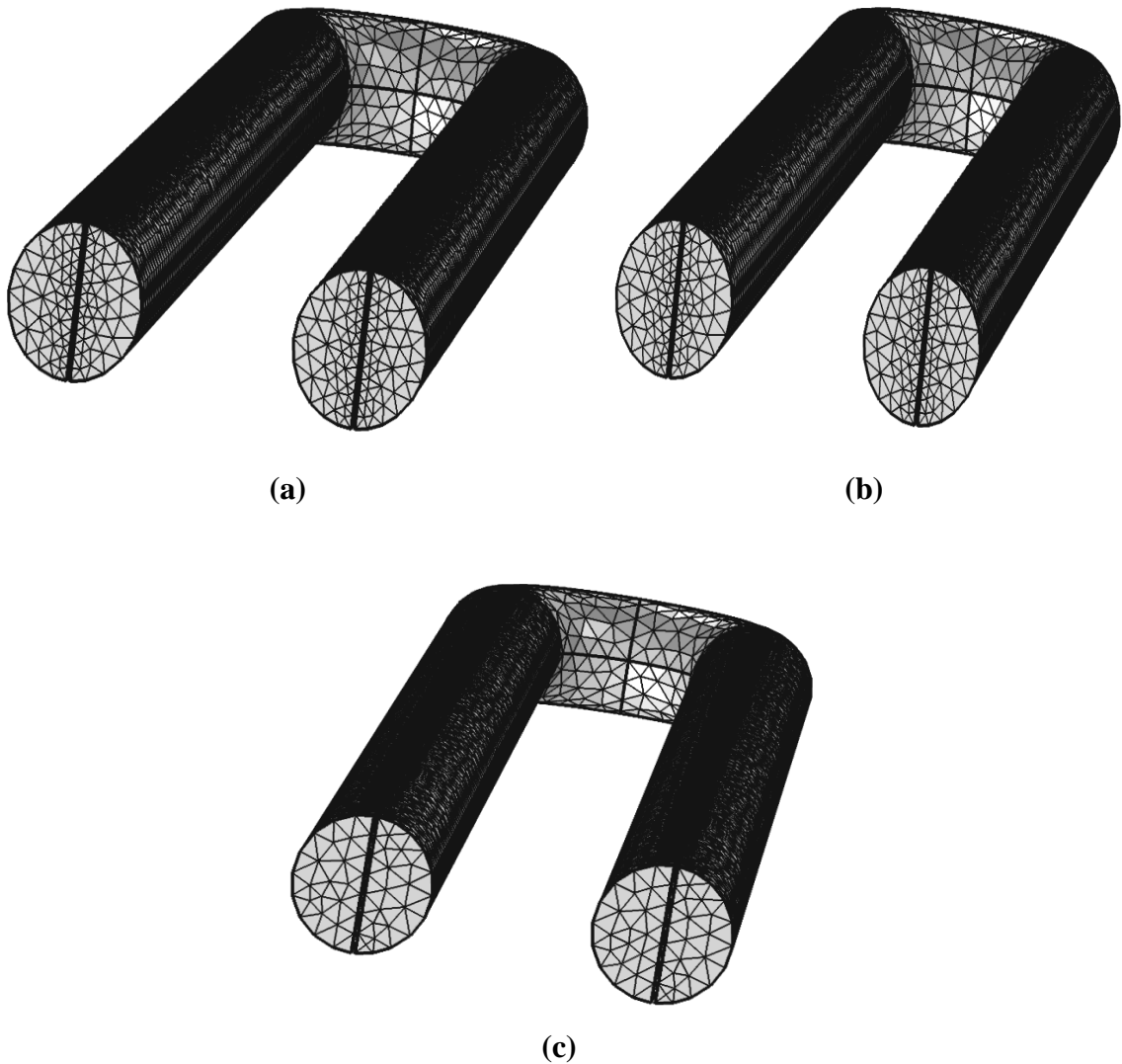


Figure 3.6: Meshing of the domain for (a) 0° angle oriented Perforated inserts tube (b) 30° angle oriented Perforated inserts tube (c) 65° angle oriented Perforated inserts tube.

Figure 3.6 displayed the massing of the domain for the angle of orientation at 0° , 30° , and 65° where finer mesh is considered to increase accuracy of the result. Around the insert and pore the mesh elements were crowded.

Table 3.1: Mesh element distribution for 65° angle oriented inserts fitted tube.

Mesh	Domain elements	Boundary elements	Edge elements	Maximum element size(mm)	Minimum element size(mm)	Remark
Normal	64640	25548	11300	171	30.8	Face is (or has a narrow region that is) much smaller than the specified minimum element size.
Fine	94826	30160	11788	137	17.1	
Finer	159046	44798	12866	94.1	6.84	Is used to with computing device.
Extra fine	1330645	172955	29572	59.9	2.57	Large amount of mesh element to compute.

For the normal and fine mesh the warning state that the face is (or has a narrow region that is) much smaller than the specified minimum element size. In this case computation doesn't held. For the extra fine mesh we consist a large amount of domain elements. It is difficult to compute such huge amount of element. For why we need to consider finer mesh for our simulation. We used MSI B85-PC-MATE motherboard with 16GB DDR3 ram based computer to compute the results.

Chapter 4

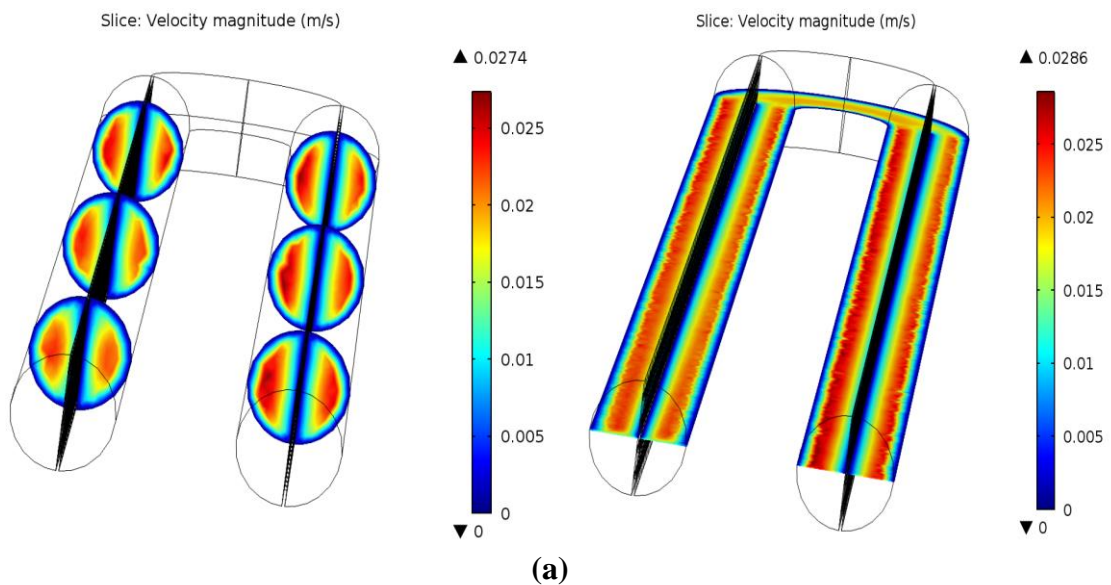
Results and discussion

4.1 Introduction

A simulation study has been carried out for heat enhancement in a pipe. A mathematical model is developed to analyze the fluid phenomena and heat augmentation. Our studies indications is to realize the heat transfer phenomena of the effect of angle oriented perforated inserts formfitting circular pipe with the simulated results. We arranged different angle of perforation of 0° , 5° , 10° , 15° , 16° , 17° , 20° , 30° , 40° , 50° , 60° , 65° , 68° and 70° correspondingly for the porosities of 4.5%, for the Reynolds number 1100, 1400 and 1700. The thickness of the copper pipe was overlooked. A constant heat flux is taken to the surfaces for the water domain. The convectional heat over the solid is neglected. The COMSOL Multiphasic software is used to compute the simulation.

4.2 Velocity profile analysis

Velocity profile of the tube for fluid flow indicate that the there is no slip condition at the wall and a high velocity in central region. It also visualizes fluid mixing quality.



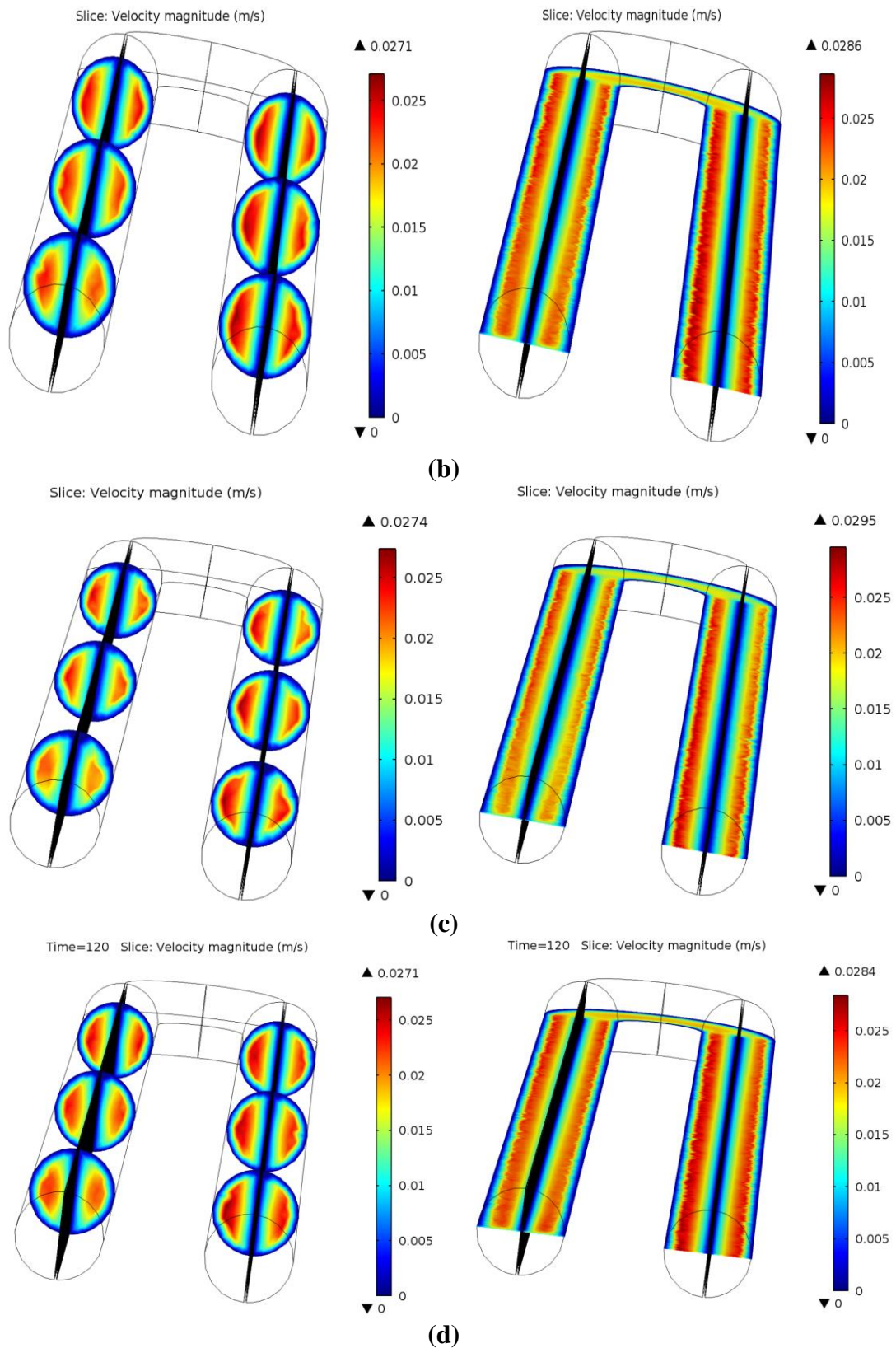
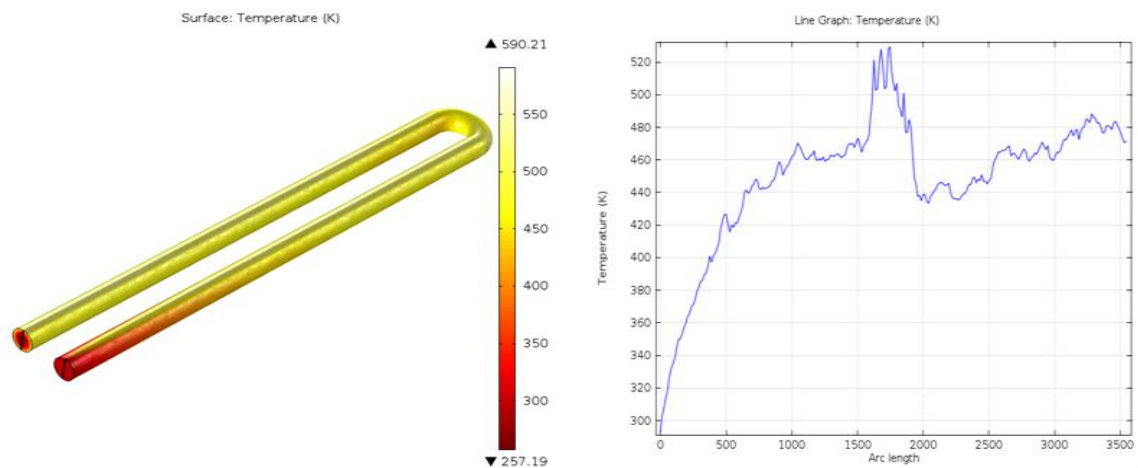


Figure 4.1: Velocity profile of the fluid for (a) 0° angle oriented Perforated inserts tube (b) 30° angle oriented Perforated inserts tube (c) 65° angle oriented Perforated inserts tube. (d) 70° angle oriented Perforated inserts tube.

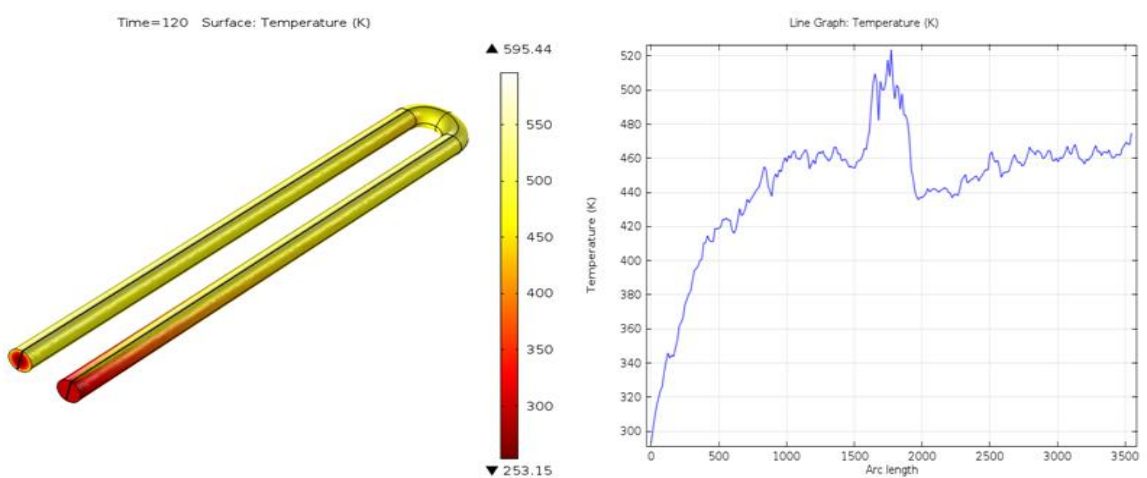
From figure 4.1 we observed that at the wall and besides the inserts the fluid velocity near to zero which visualize by blue region and the fluid velocity gradually high at the center between wall and inserts is showed by turn to red region. This also shows that the fluid particle mix well at figure 4.1(c) than figure 4.1(a), figure 4.1(b) and figure 4.1(d).

4.3 Temperature Augmentation Assessment

The perforated inserts pipe augmented more heat than the without insert fitted pipe or plane pipe is noted by [Bhuiya M. M. K. et.al. \(2012\)](#) and [Acherjee S. et.al. \(2017\)](#).



(a)



(b)

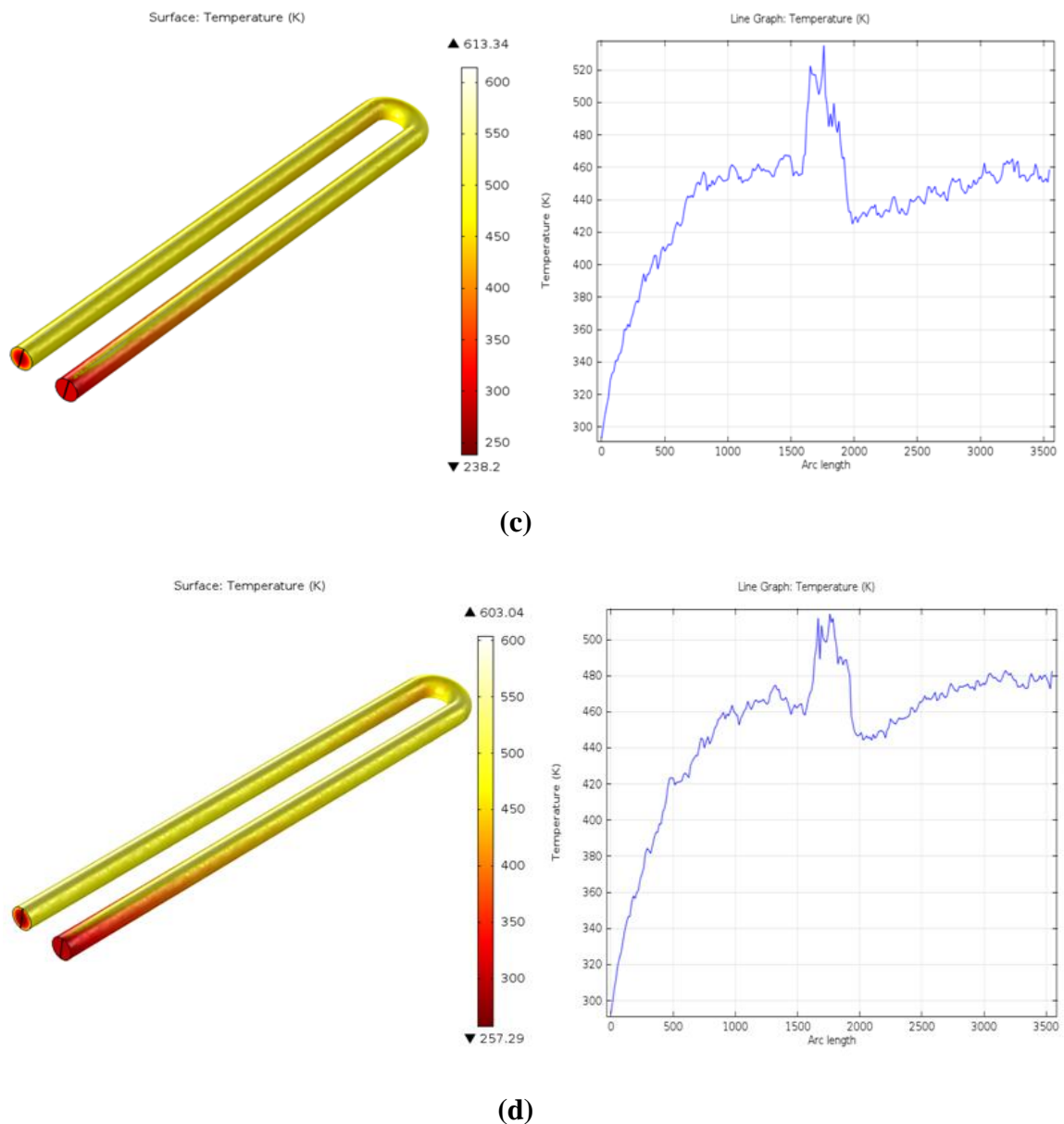


Figure 4.2: Surface temperature and temperature line graph of the fluid for (a) 0° angle oriented Perforated inserts tube (b) 30° angle oriented Perforated inserts tube (c) 65° angle oriented Perforated inserts tube (d) 70° angle oriented Perforated inserts tube.

Figure 4.2 described a round pipe with angle arranged axial perforated inserts (figure 4.2(b), 4.2(c) and 4.2(d)) shows better result in case of heat transfer than the general axial perforated inserts (figure 4.2(a)). The path line for the fluid particle at various angle oriented axial perforated inserts pipe can easily create curves which influence to

increase the temperature. On the other hand, regular perforated axial inserts pipe unable to create more curves with the streamline for the fluid particle for what the heat transfer augmentation remains low. Which are analyzed in details in the following sections.

4.4 Wall temperature and Bulk temperature analysis

The temperature slice at three different position for four different angle oriented tube is displayed below.

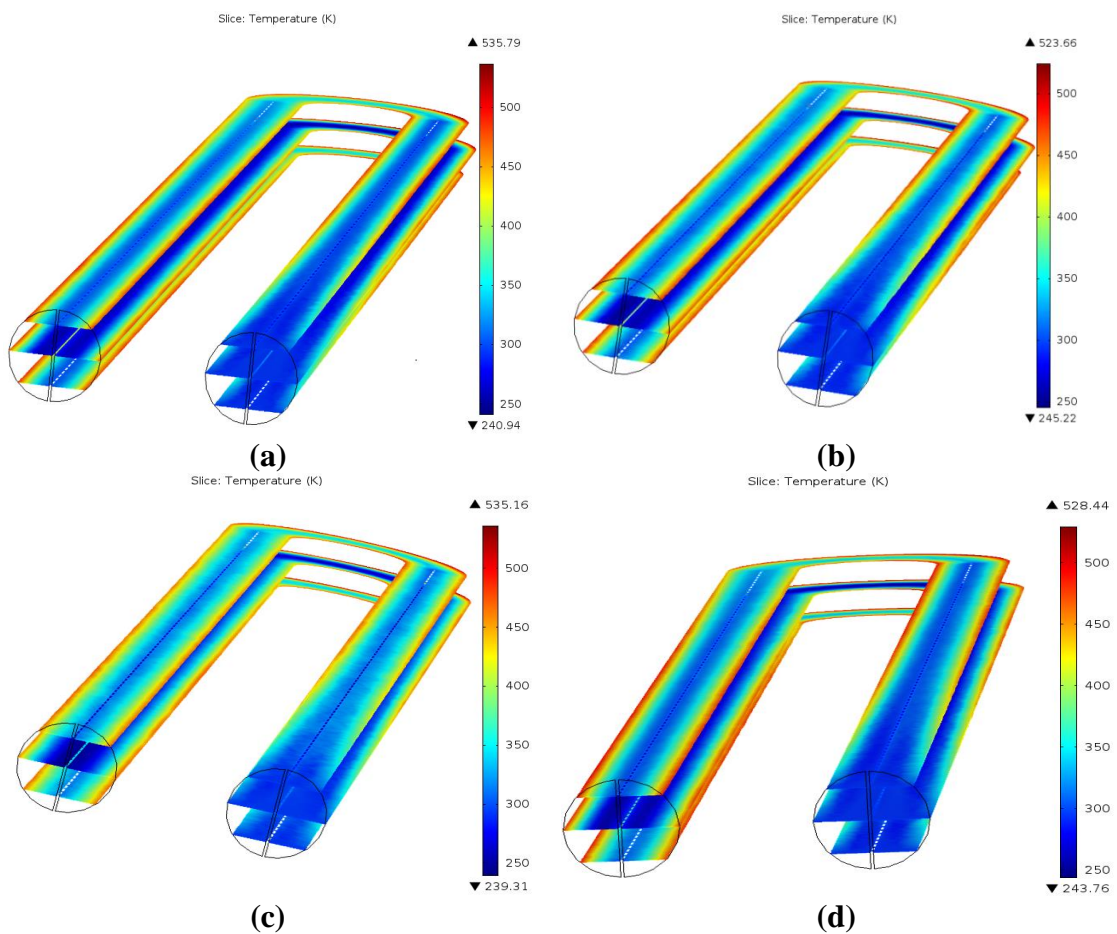
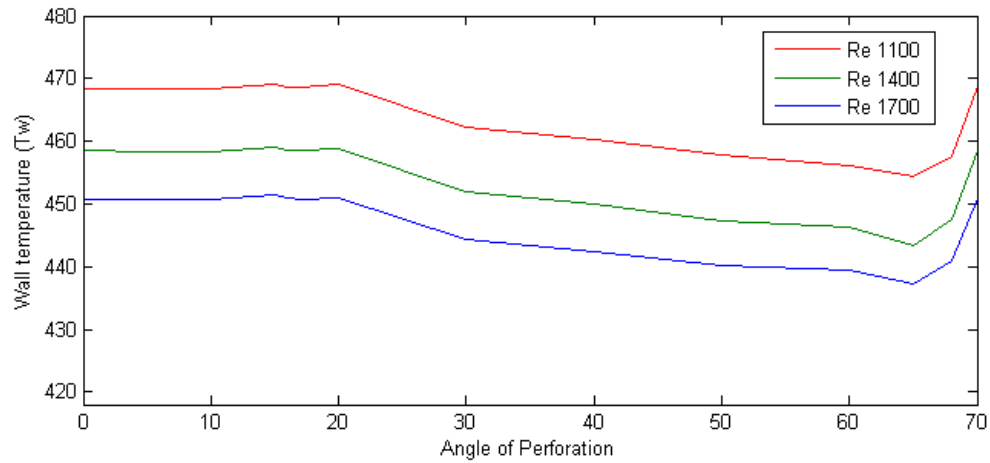
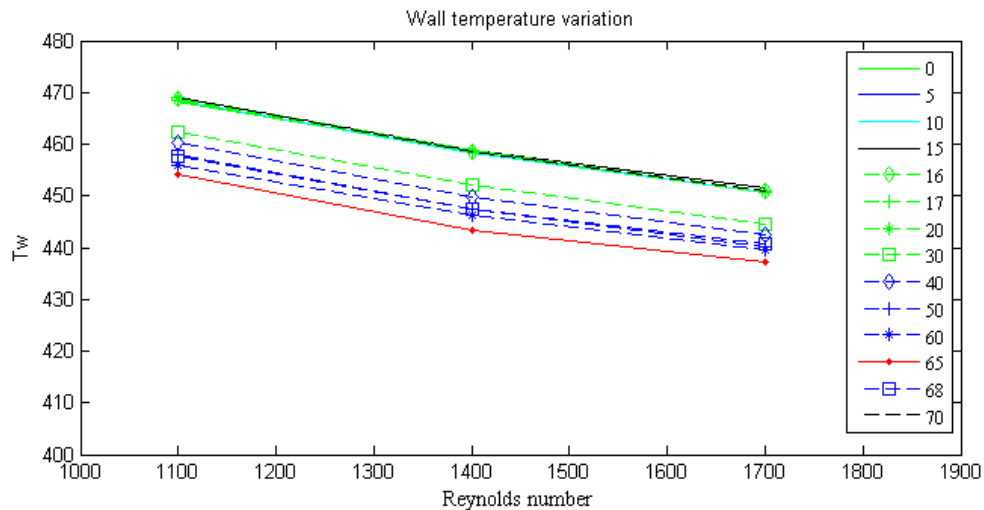


Figure 4.3: Bulk temperature phenomena of the fluid for (a) 0° angle oriented Perforated inserts tube (b) 30° angle oriented Perforated inserts tube (c) 65° angle oriented Perforated inserts tube (d) 70° angle oriented Perforated inserts tube.

Figure 4.3 shows that in figure 4.3(c) the heated fluid particle from the surface mix very well with the core particle and transfer more heat to the bulk fluid than figure 4.1(a), figure 4.1(b) and figure 4.1(d).



(a)



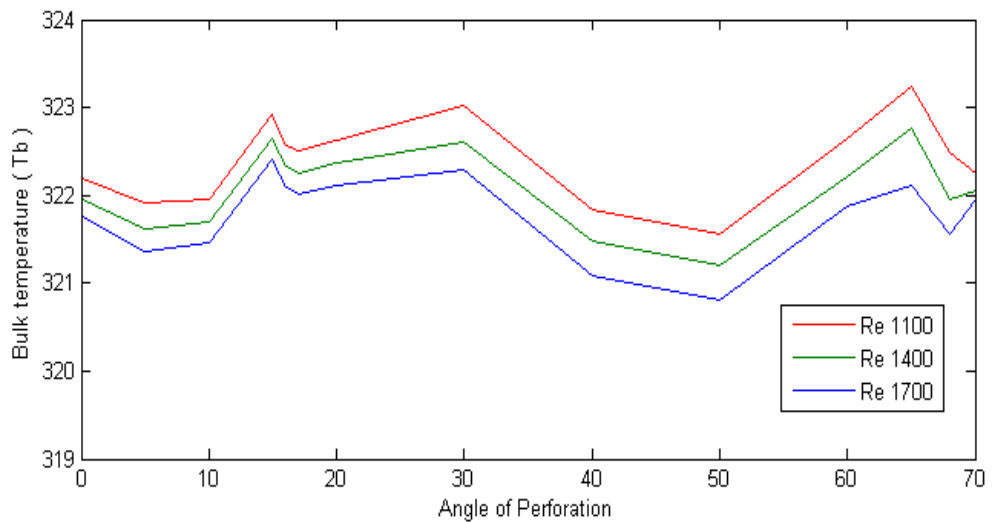
(b)

Figure 4.4: Wall temperature graph of the fluid at different angle oriented inserts for different Reynolds number.

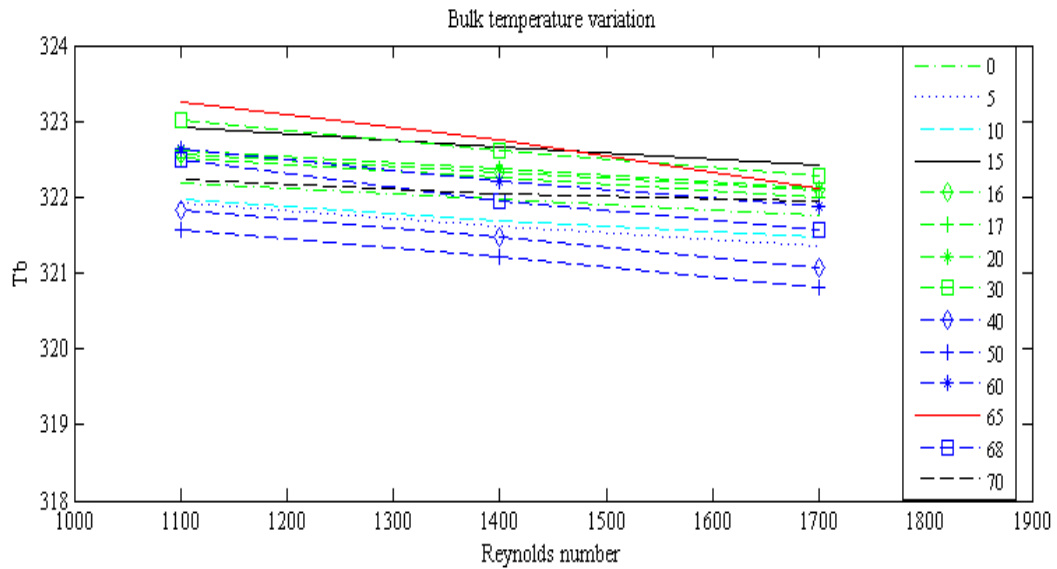
The Figure 4.4 represents the wall temperature for different Reynolds number along with the bulk temperature at different angle oriented of perforation 0° , 5° , 10° , 15° , 16° , 17° , 20° , 30° , 40° , 50° , 60° , 65° , 68° and 70° . From the figure 4.4(a), 4.4(b) and table 4.1 it is clear that the wall temperature for 65° angle oriented insert fitted tube is remains low for all Reynolds number.

Table 4.1: Wall temperature data of the domain at different angle oriented inserts for different Reynolds number.

	Re = 1100	Re = 1400	Re = 1700
0°	468.25214	458.51547	450.74326
5°	468.43925	458.31311	450.66122
10°	468.39947	458.26849	450.69006
15°	469.19476	458.97355	451.41688
16°	468.68229	458.57687	451.0049
17°	468.54722	458.46762	450.72673
20°	469.02723	458.84003	450.97853
30°	462.22861	452.0494	444.42126
40°	460.33288	449.91019	442.40629
50°	457.87818	447.36041	440.10493
60°	456.0123	446.22663	439.42303
65°	454.29888	443.27871	437.22384
68°	457.57135	447.5887	440.83017
70°	468.90868	458.49935	451.06627



(a)



(b)

Figure 4.5: Variation of bulk temperature at different angle oriented inserts for different Reynolds number.

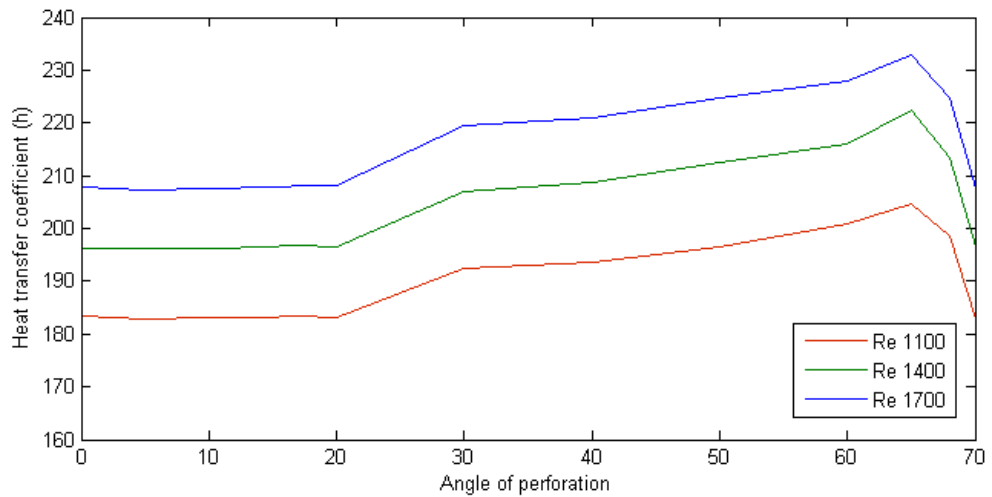
The bulk temperature at different angle oriented inserts of perforation 0° , 5° , 10° , 15° , 16° , 17° , 20° , 30° , 40° , 50° , 60° , 65° , 68° and 70° for different Reynolds number is characterizes by the Figure 4.5. From the Figure 4.5(a), 4.5(b) and the Table 4.2 we noted that the bulk temperature for 65° angle oriented insert fitted tube is remains high for the Reynolds number 1100 and 1400. For the Reynolds number 1700 the highest value comes from 15° angle oriented insert fitted tube. It also added that the lower wall temperature leads to higher bulk temperature.

Table 4.2: Bulk temperature data of the domain at different angle oriented inserts for different Reynolds number.

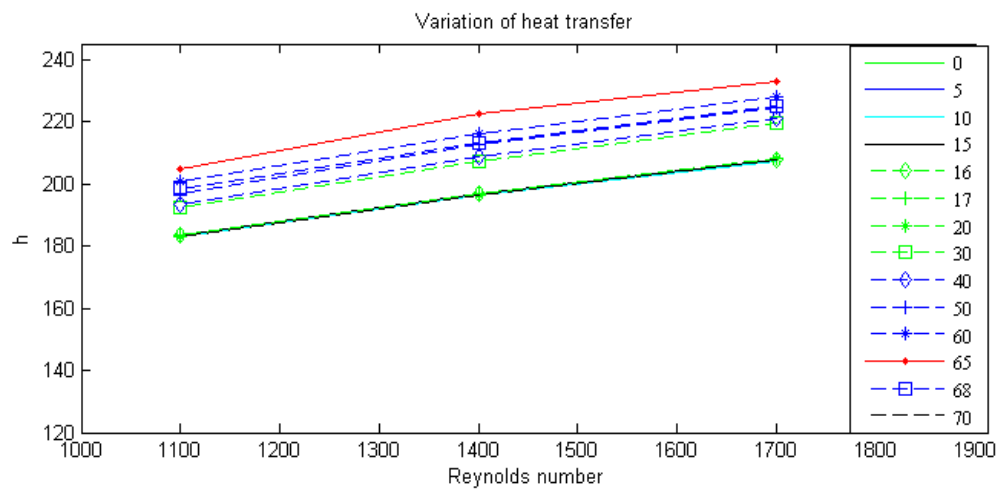
	Re = 1100	Re = 1400	Re = 1700
0°	322.19688	321.96814	321.75569
5°	321.91316	321.61501	321.36656
10°	321.96332	321.68957	321.46876
15°	322.91844	322.64908	322.41143
16°	322.57675	322.32704	322.0932
17°	322.51075	322.25109	322.00755
20°	322.62364	322.37137	322.11793
30°	323.0132	322.60866	322.28985
40°	321.8418	321.47477	321.08196
50°	321.55735	321.21104	320.80336
60°	322.64026	322.20333	321.88175
65°	323.24441	322.75928	322.1169
68°	322.48321	321.95656	321.56861
70°	322.24443	322.04506	321.96034

4.5 Heat transfer coefficient analysis

The value of heat transfer coefficient indicates the heat transfer augmentation of a heat transfer device.



(a)



(b)

Figure 4.6: Variation of heat transfer coefficient at different angle oriented inserts for different Reynolds number.

The variation of heat transfer coefficient at different angle oriented inserts for different Reynolds number represents in the Figure 4.6. Here we observed from the Figure 4.6(a), 4.6(b), and the Table 4.3 that for the 65° angle oriented perforated inserts tube the heat transfer coefficient obtain the highest value than the other angle oriented inserts for different Reynolds number.

Table 4.3: Heat transfer coefficient data of the domain at different angle oriented inserts for different Reynolds number.

	Re = 1100	Re = 1400	Re = 1700
0°	183.5345	196.314194	207.81987
5°	182.944751	196.097678	207.326265
10°	183.057121	196.268795	207.443974
15°	183.25714	196.635124	207.791066
16°	183.471339	196.742851	207.942173
17°	183.558115	196.79094	208.253191
20°	183.097826	196.42737	208.024633
30°	192.551816	207.092296	219.486362
40°	193.558892	208.713297	220.94645
50°	196.640381	212.495552	224.692591
60°	200.987996	216.138249	228.057581
65°	204.542279	222.422061	232.880659
68°	198.43474	213.3704	224.767971
70°	182.772414	196.448049	207.629339

4.6 Wall temperature and Heat transfer coefficient relation

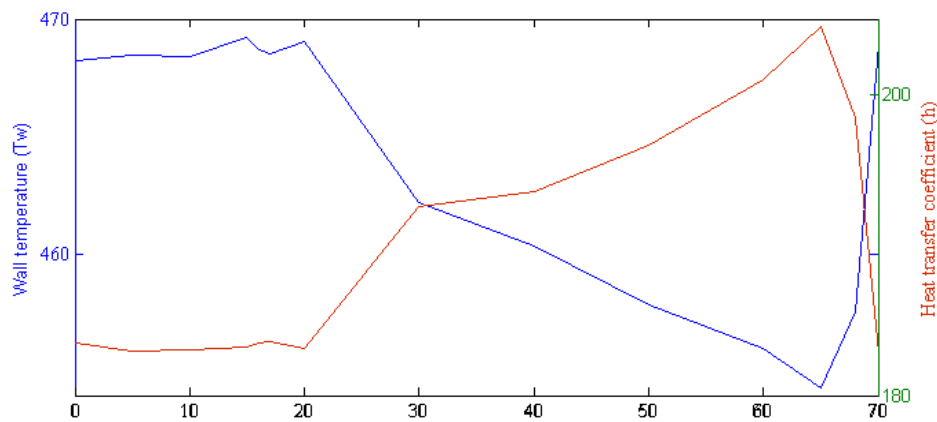


Figure 4.7: The comparison of wall temperature and heat transfer coefficient for the different angle of perforation.

The Figure 4.7 describes the contrast of heat transfer coefficient and wall temperature for the Reynolds number 1100. From the Figure 4.7 we notice that the wall temperature varies inversely with the heat transfer coefficient. The Table 4.4 also note the same scenario for the Reynolds number 1100, 1400 and 1700. This is because when the fluid particles get enough facility to mix and transfer heat to the core

particles of the tube then the surface temperature remains decreased with the increasing of heat transfer coefficient else it acts reversely

Table 4.4: The comparison of wall temperature and heat transfer coefficient for the different angle of perforation.

	Re = 1100		Re = 1400		Re = 1700	
	T_w	h	T_w	h	T_w	h
0°	468.25214	183.5345	458.51547	196.314194	450.74326	207.81987
5°	468.43925	182.944751	458.31311	196.097678	450.66122	207.326265
10°	468.39947	183.057121	458.26849	196.268795	450.69006	207.443974
15°	469.19476	183.25714	458.97355	196.635124	451.41688	207.791066
16°	468.68229	183.471339	458.57687	196.742851	451.0049	207.942173
17°	468.54722	183.558115	458.46762	196.79094	450.72673	208.253191
20°	469.02723	183.097826	458.84003	196.42737	450.97853	208.024633
30°	462.22861	192.551816	452.0494	207.092296	444.42126	219.486362
40°	460.33288	193.558892	449.91019	208.713297	442.40629	220.94645
50°	457.87818	196.640381	447.36041	212.495552	440.10493	224.692591
60°	456.0123	200.987996	446.22663	216.138249	439.42303	228.057581
65°	454.29888	204.542279	443.27871	222.422061	437.22384	232.880659
68°	457.57135	198.43474	447.5887	213.3704	440.83017	224.767971
70°	468.90868	182.772414	458.49935	196.448049	451.06627	207.629339

4.7 Nusselt number Performance Evaluation.

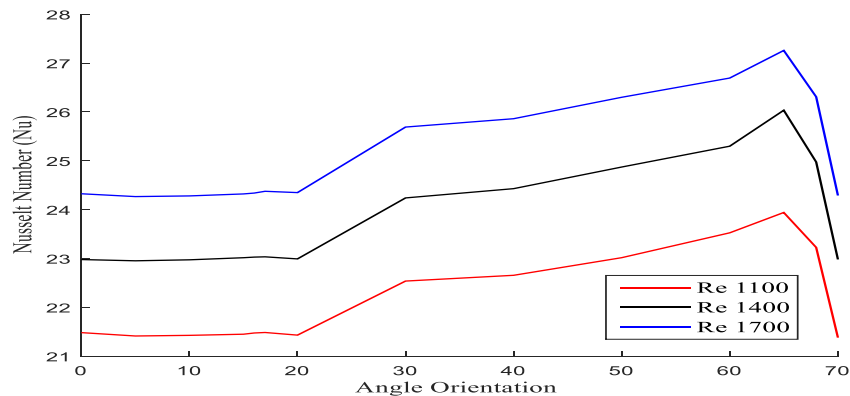


Figure 4.8: Nusselt number variation with Reynolds number for the different angle of perforation.

The relationship between the Nusselt number and the Reynolds number is depicted in the Figure 4.8 and the Table 4.5. We observed that the Nusselt number varies with the Reynolds number. Nusselt number is increased for all angles of perforated inserts with the increasing of Reynolds number. From the figure. 4.8 we detected a sharp

drop of Nusselt number after 65° to 70° angle oriented tube. The maximum value of Nusselt number is found for the angle of perforation 65° at all Reynolds numbers. The reason behind this the fluid particle might move rapidly at 68° and 70° compare to 65° degree. So the fluid particles do not get enough time to transmit heat to the core particles of the fluid in the tube for why the Nusselt number decreased gradually.

Table 4.5: Nusselt number data of the domain at different angle oriented inserts for different Reynolds number.

	Re = 1100	Re = 1400	Re = 1700
0°	21.4828938	22.9787696	24.3255203
5°	21.4138632	22.9534262	24.2677434
10°	21.4270161	22.9734556	24.2815213
15°	21.4504285	23.0163347	24.3221488
16°	21.4755008	23.0289443	24.3398359
17°	21.4856579	23.0345732	24.376241
20°	21.4317807	22.992017	24.3494879
30°	22.5383795	24.240357	25.6910947
40°	22.6562588	24.4300968	25.8619994
50°	23.0169501	24.8728135	26.3004889
60°	23.5258427	25.2991948	26.6943643
65°	23.9418751	26.0347211	27.2589103
68°	23.2269816	24.9752153	26.3093122
70°	21.393691	22.9944374	24.3032185

4.8 Nusselt number and Heat transfer coefficient relation

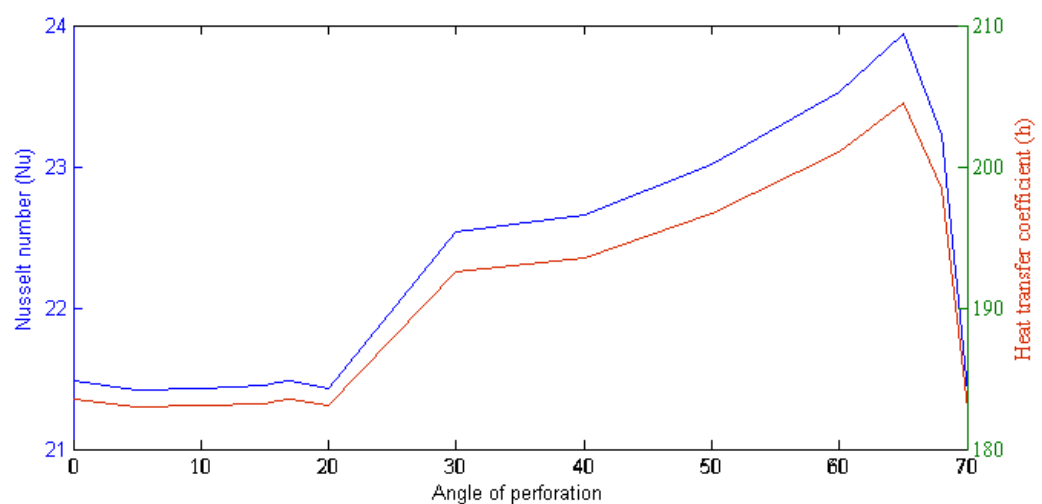


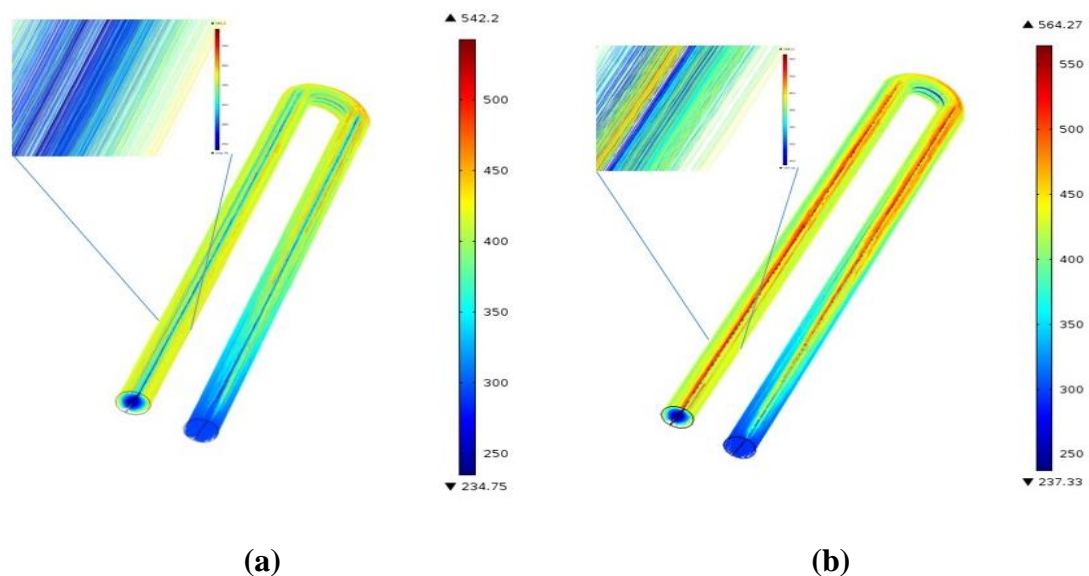
Figure 4.9: Nusselt number and heat transfer relation for the different angle of perforation.

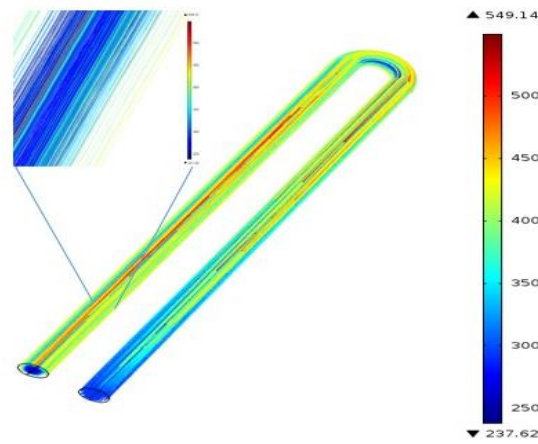
Nusselt number and heat transfer relation for the different angle of perforation for the Reynolds number 1100 described by the Figure 4.9 and the Table 4.6 represents the data at the same relation for the Reynolds number 1100, 1400 and 1700. This figure shows us the Nusselt number is proportional with the heat transfer coefficient. Table 4.6 indicates the same for the Reynolds number 1400 and 1700. Nusselt number is increased with the increasing of heat transfer coefficient.

Table 4.6: Nusselt number and heat transfer relation data for the different angle of perforation.

	Re = 1100		Re = 1400		Re = 1700	
	N_u	h	N_u	h	N_u	h
0°	21.4828938	183.5345	22.9787696	196.314194	24.3255203	207.81987
5°	21.4138632	182.944751	22.9534262	196.097678	24.2677434	207.326265
10°	21.4270161	183.057121	22.9734556	196.268795	24.2815213	207.443974
15°	21.4504285	183.25714	23.0163347	196.635124	24.3221488	207.791066
16°	21.4755008	183.471339	23.0289443	196.742851	24.3398359	207.942173
17°	21.4856579	183.558115	23.0345732	196.79094	24.376241	208.253191
20°	21.4317807	183.097826	22.992017	196.42737	24.3494879	208.024633
30°	22.5383795	192.551816	24.240357	207.092296	25.6910947	219.486362
40°	22.6562588	193.558892	24.4300968	208.713297	25.8619994	220.94645
50°	23.0169501	196.640381	24.8728135	212.495552	26.3004889	224.692591
60°	23.5258427	200.987996	25.2991948	216.138249	26.6943643	228.057581
65°	23.9418751	204.542279	26.0347211	222.422061	27.2589103	232.880659
68°	23.2269816	198.43474	24.9752153	213.3704	26.3093122	224.767971
70°	21.393691	182.772414	22.9944374	196.448049	24.3032185	207.629339

4.9 Streamline phenomena



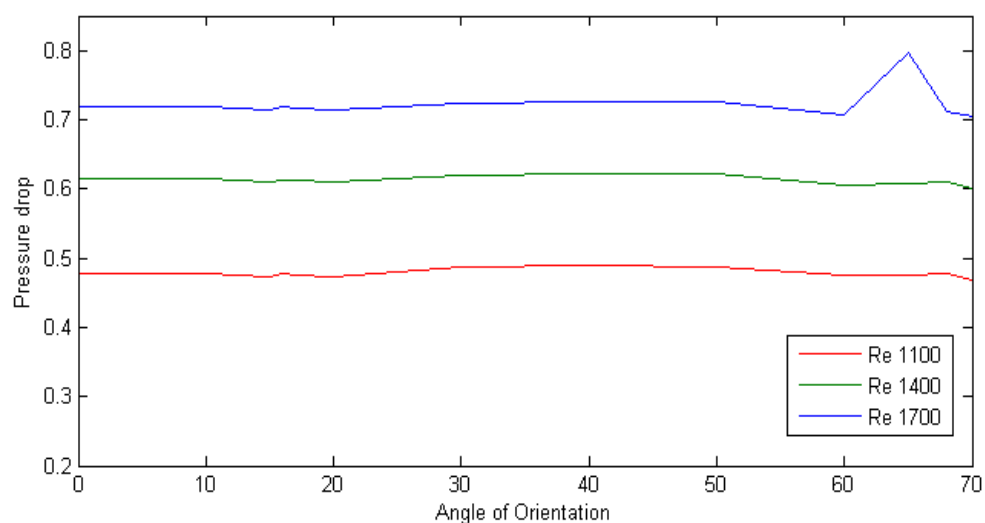


(c)

Figure 4.10: Streamline phenomena of the fluid for (a) 68° angle oriented Perforated inserts tube (b) 65° angle oriented perforated inserts tube (c) 70° angle oriented perforated inserts tube.

The performance of the streamline phenomena for 65° , 68° and 70° angle oriented perforated inserts tube is exposed in the Figure 4.10. Such kind of illustration of Figure 4.10(a) and Figure 4.10(c) detected us that an amount of highly heated fluid particles near to the wall and a huge amount of lower heated particle at the core for 68° and 70° angle oriented perforated inserts tube. On the other hand, at the Figure 4.10(b) for 65° angle oriented perforated inserts tube the color of path line of fluid particle indicate the mixing of heated particles with the core particles.

4.10 Pressure drop distribution



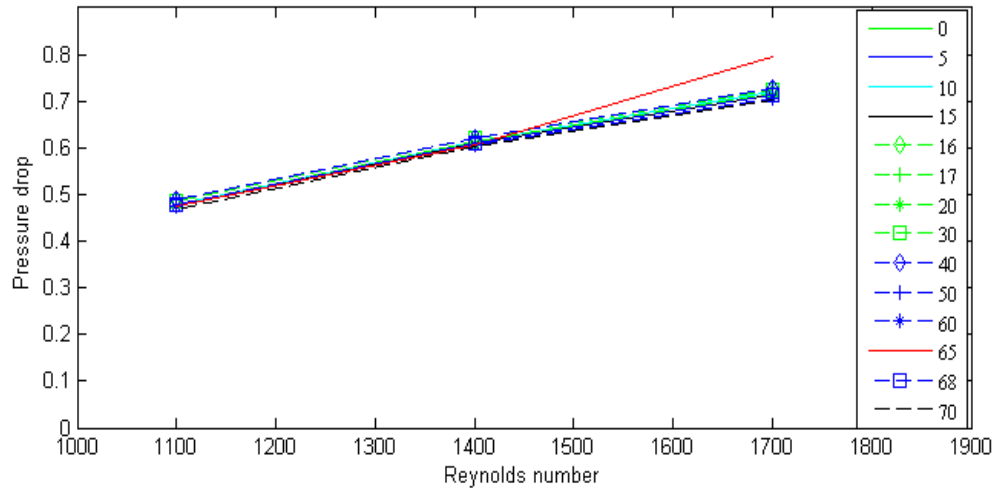


Figure 4.11: Pressure drop distribution of the fluid at different angle oriented inserts for different Reynolds number.

Pressure drop indicates the friction of fluid particle, if there were no friction then the pressure drop would be zero. For rough surface the drop of pressure remains high. The friction factor can be calculated from the pressure drop. The Figure 4.11 and the Table 4.7 represents the distribution of pressure drop of fluid flow for the Reynolds number at various angle oriented inserts.

Table 4.7: Pressure drop distribution data of the fluid at different angle oriented inserts for different Reynolds number.

	Re = 1100	Re = 1400	Re = 1700
0°	0.47752	0.61413	0.71924
5°	0.47746	0.61392	0.71906
10°	0.4779	0.61454	0.71948
15°	0.47396	0.60975	0.714
16°	0.47691	0.61322	0.71796
17°	0.47633	0.6125	0.71738
20°	0.47404	0.61023	0.71493
30°	0.48735	0.62003	0.72377
40°	0.48934	0.62233	0.72653
50°	0.48816	0.62196	0.72646
60°	0.47517	0.60535	0.706
65°	0.47568	0.60766	0.79672
68°	0.47766	0.60959	0.712
70°	0.46811	0.60121	0.70392

4.11 Friction Factor Performance Evaluation

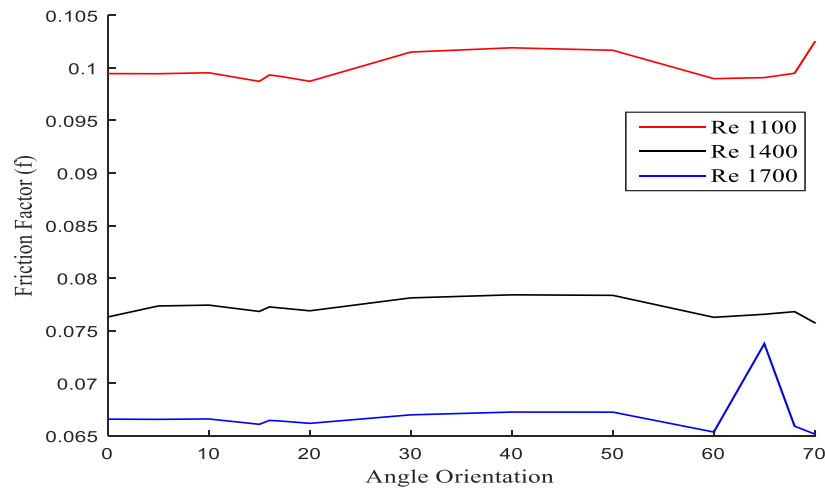


Figure 4.12: Friction factor variation with Reynolds number for the different angle of perforation.

From the Figure 4.12 we observed that the friction factor is decreased with the increasing of the Reynolds number. The friction factor is diverges with the variation of angle. The friction factor rises at the angle of 30° to 50° and then it showed a downward trend till to 60° . The Table 4.8 represents the data for this phenomena, where we observed that the highest value comes from 40° angle oriented tube for the Reynolds number 1100 and 1400. While at the Reynolds number 1700 it's comes from 65° angle oriented tube.

Table 4.8: Friction factor variation data with Reynolds number for the different angle of perforation.

	Re = 1100	Re = 1400	Re = 1700
0°	0.09945992	0.077379775	0.066580576
5°	0.09944742	0.077353315	0.066563913
10°	0.09953907	0.077431434	0.066602793
15°	0.09871843	0.076827899	0.066095505
16°	0.09933287	0.077265116	0.066462085
17°	0.09921206	0.077174396	0.066408394
20°	0.09873509	0.076888379	0.066181596
30°	0.10150735	0.078123169	0.066999921
40°	0.10192184	0.078412967	0.067255417
50°	0.10167606	0.078366347	0.067248937
60°	0.09897045	0.076273504	0.065354939
65°	0.09907668	0.076564561	0.073752956
68°	0.09948908	0.076807739	0.065910364
70°	0.09749996	0.075751868	0.065162392

4.12 Friction Factor and Pressure drop relation

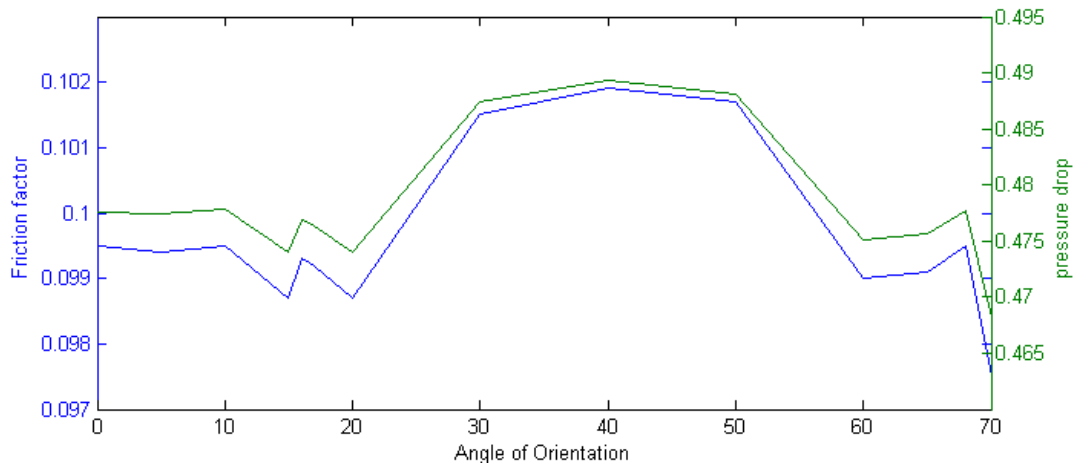


Figure 4.13: Friction factor and pressure drop relation for the different angle of perforation.

The relation between friction factor and pressure drop for the different angle of perforation displays by the Figure 4.13 for the Reynolds number 1100. The data for the same relation with the Reynolds number 1100, 1400 and 1700 were represents in the Table 4.9. This illustration shows us friction factor increases with the increasing of pressure drop.

Table 4.9: Friction factor and pressure drop relation for the different angle of perforation.

	Re = 1100		Re = 1400		Re = 1700	
	f	ΔP	f	ΔP	f	ΔP
0°	0.09945992	0.47752	0.077379775	0.61413	0.066580576	0.71924
5°	0.09944742	0.47746	0.077353315	0.61392	0.066563913	0.71906
10°	0.09953907	0.4779	0.077431434	0.61454	0.066602793	0.71948
15°	0.09871843	0.47396	0.076827899	0.60975	0.066095505	0.714
16°	0.09933287	0.47691	0.077265116	0.61322	0.066462085	0.71796
17°	0.09921206	0.47633	0.077174396	0.6125	0.066408394	0.71738
20°	0.09873509	0.47404	0.076888379	0.61023	0.066181596	0.71493
30°	0.10150735	0.48735	0.078123169	0.62003	0.066999921	0.72377
40°	0.10192184	0.48934	0.078412967	0.62233	0.067255417	0.72653
50°	0.10167606	0.48816	0.078366347	0.62196	0.067248937	0.72646
60°	0.09897045	0.47517	0.076273504	0.60535	0.065354939	0.706
65°	0.09907668	0.47568	0.076564561	0.60766	0.073752956	0.79672
68°	0.09948908	0.47766	0.076807739	0.60959	0.065910364	0.712
70°	0.09749996	0.46811	0.075751868	0.60121	0.065162392	0.70392

4.13 Thermal Performance Criterion

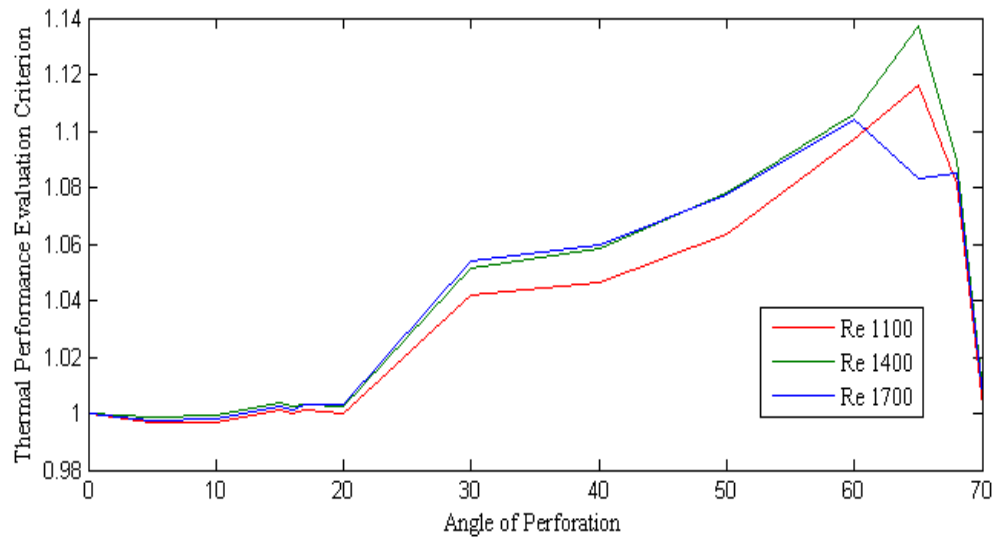


Figure 4.14: Thermal performance variation with Reynolds number for the different angle of perforation.

Thermal performance evaluation criterion defines the performance of the device. The Figure 4.14 illustrate the visual phenomena and the Table 4.10 describes the data for the illustration of thermal Performance Evaluation Criterion.

Table 4.10: Data of thermal performance variation with Reynolds number for the different angle of perforation.

	Re = 1100	Re = 1400	Re = 1700
0°	1	1	1
5°	0.99682847	0.99901098	0.99770808
10°	0.99713454	0.99954636	0.99808024
15°	1.0009825	1.00402739	1.00230141
16°	1.00008189	1.00267902	1.00118278
17°	1.00096084	1.00331693	1.00295039
20°	1.00005603	1.00270355	1.00299276
30°	1.04202972	1.0515456	1.05392949
40°	1.04605784	1.05846933	1.05959537
50°	1.06356684	1.07786432	1.07759539
60°	1.09689887	1.10627861	1.10419851
65°	1.11589741	1.13699716	1.08301812
68°	1.08107932	1.08957375	1.08520546
70°	1.00247639	1.00779931	1.0062792

The highest thermal performance evaluation criterion is found at the different angle oriented inserts for 65° perforation angle with the Reynolds number of 1100 and 1400. Though, for the Reynolds number of 1700 the maximum PEC is observed for the 60° of perforated angle oriented tube. Furthermore, the uppermost value is found for the Reynolds number of 1400 with angle of perforation 65° .

At the Reynolds number of 1100 the thermal performance evaluation criterion is found 1.09, 1.10 and 1.08 times higher for the angle of perforation of 60° , 65° and 68° than the regular axial perforated inserts fitted tube.

The thermal performance evaluation criterion gives 1.106, 1.136 and 1.089 times greater for the angle of perforation of 60° , 65° and 68° than the regular axial perforated inserts fitted tube or 0° perforated inserts fitted tube is found for the Reynolds number of 1400.

At the Reynolds number of 1700 the thermal performance evaluation criterion is noted 1.104, 1.083 and 1.085 times better for the angle of perforation of 60° , 65° and 68° than the 0° angle oriented perforated inserts fitted tube.

Chapter 5

Conclusion and Recommendation

5.1 Conclusion

In our study we investigated a CFD simulation study of the heat transfer analysis with perforated insert using different angle of perforation in a circular pipe. To analyze the heat transfer phenomena we considered with 14 different angle (0° , 5° , 10° , 15° , 16° , 17° , 18° , 20° , 30° , 40° , 50° , 60° , 65° , 68° and 70°) oriented perforated inserts for a pipe. A constant heat-flux around the tube is assumed for our simulations.

At the perforation angle of 0° the streamline of the fluid particle do not make enough obstacle to create swirl. However it is easy to create swirl in higher degree angle oriented axial perforated inserts tube which increased the temperature of the fluid. Here it is seen that the bulk fluid temperature mix well with the fluid for 65° angle oriented perforated insert tube than any other angle oriented tube.

From our study, It also noted that the lower wall temperature of the tube influence the higher bulk temperature for the fluid.

We observed that the highest heat transfer rate is counted for 65° angle oriented Perforated inserts tube than the other angle oriented inserts for different Reynolds numbers.

We also found that the wall temperature varies inversely with the heat transfer rate while fluid flows inside the pipe.

The Nusselt number and thermal Performance Evaluation Criterion tends to be higher is found at the 65° angle oriented perforated inserts tube, than all other angles measured in our model.

The Nusselt number is obtained 1.11 to 1.13 times for the 65° angle oriented perforated inserts. In all Reynolds numbers the highest Nusselt number is found for the angle of perforation 65° . Though, subsequently the Nusselt number displays a sharp fall around 65° to 70° .

It is also observed that the fluid temperature varies inversely up to a saturated level with the gradual increase of high Reynolds number for all angles of perforated inserts.

At the Reynolds number of 1100 the thermal performance evaluation criterion is found 1.10 times higher for the angle of perforation of 65° than the regular axial perforated inserts fitted tube.

The thermal performance evaluation criterion gives 1.136 times greater for the angle of perforation of 65° compare to 0° perforated inserts fitted tube while the Reynolds number is around 1400.

At the Reynolds number of 1700 the thermal performance evaluation criterion is noted 1.104 times better for the angle of perforation of 60° than 0° angle oriented perforated inserts fitted tube.

5.2 Recommendation for future work

A numerical simulation of heat transfer using different angle of perforation in perforated insert are studies in our present work. In this work we use water, as acting fluid in a u-loop circular pipe with axial inserts. Our recommendation for future works are given below:

- One can run through their investigation with experimental setup.
- Square, rectangular, triangular and any other duct can be used instead of circular duct.
- Investigation for turbulent flow can also be investigated for better prediction.
- MDH fluid may be used instead of water as compared with application sectors.

References

- Acherjee S., Shahriar M., Bhuyan M.M., Deb U. K., Enhancement Of Heat Transfer In A U-Loop Circular Tube With Axial Perforated Inserts, Southeast-Asian J. of Sciences, 2017, vol. 5, no. 2, pp. 126-136.
- Ahamed J. U., Wazed M. A., Ahmed S., Nukman Y., Tuan Ya T. M. Y. S., and Sarkar M. A. R., Enhancement and Prediction of Heat Transfer Rate in Turbulent Flow Through Tube with Perforated Twisted Tape Inserts: A New Correlation, Journal of Heat Transfer, Transactions of the ASME 2011, vol.133, pp.0419031-9.
- Ahamed J. U., Wazed M.A., Ahmed S., Sarkar M.A.R., Enhancement of heat transfer in turbulent flow through a tube with a perforated twisted tape insert, Proceedings of the International Conference on Mechanical Engineering 2007 (ICME2007), Bangladesh.
- Bergman, T. L. Fundamentals of heat and mass transfer. John Wiley & Sons. 2011.
- Bhattacharyya S., Roy T., Ghosh N., Bandyopadhyay S., Sarkar S., Panja P., convective heat transfer enhancement in low Reynolds number of a circular pipe with full length twisted tape insert, Proceedings of 12th IRF International Conference, 2014, India.
- Bhuiya M. M. K., Ahamed J. U., Sarkar M. A. R., Salam B., Masjuki H. H., Kalam M.A., Saidur R., Sayem A. S. M. Heat Transfer and Pressure Drop Characteristics in Turbulent Flow Through a Tube, Experimental Heat Transfer: A Journal of Thermal Energy Generation, Transport, Storage, and Conversion, 2012, vol. 25, no. 4, pp. 301-322.
- Bhuiya M.M.K., Chowdhury M.S.U., Saha M., Islam M.T., Heat transfer and friction factor characteristics in turbulent flow through a tube fitted with perforated twisted tape inserts, International Communications in Heat and Mass Transfer, 2013, vol. 46, pp.49–57.
- Bhuyan M. M., Deb U. K., Shahriar M., Acherjee S., Simulation of heat transfer in a tubular U-loop pipe using the rectangular inserts and without insert, AIP Conference Proceedings 2017, 1851, pp. 020011-8.
- Bhuyan M. M., Deb U. K., Shahriar M., Acherjee S., Simulation of Heat Transfer in a Tubular Pipe Using Different Twisted Tape Inserts, Open Journal of Fluid Dynamics, 2017, vol. 7, pp. 397-409
- Bhuiya M.M.K, An experimental study of heat transfer in turbulent flow through a tube fitted with perforated rectangular strip insert. M.Sc. Thesis, Department of Mechanical Engineering, BUET, Bangladesh.

Chowdhuri, M. A. K., Hossain, R. A., & Sarkar, M. A. R. An experimental investigation of turbulent flow heat transfer through tube with rod-pin insert. *International Journal of Engineering, Science and Technology*, 2011, vol. 3 no.4.

Chen L. Finite Volume Method, <https://www.math.uci.edu/~chenlong/226/FVM.pdf>

Ciarlet, P. G., & Lions, J. L. (Eds.). *Handbook of Numerical Analysis: Solution of Equations in R^n (Part 4), Techniques of Scientific Computer (Part 4), Numerical Methods for Fluids (Part 2) 1990 Vol. 8.* Gulf Professional Publishing 1990.

Date, A. W., & Gaitonde, U. N. Development of correlations for predicting characteristics of laminar flow in a tube fitted with regularly spaced twisted-tape elements. *Experimental Thermal and Fluid Science*, 1990, vol. 3, no. 4, pp. 373-382.

Eiamsa-ard, S., Wongcharee, K., Eiamsa-Ard, P., & Thianpong, C. Heat transfer enhancement in a tube using delta-winglet twisted tape inserts. *Applied Thermal Engineering*, 2010, vol. 30, no. 4, pp. 310-318.

El-Shamy, A. R. Turbulent flow and convective heat transfer in an Annulus with perforated disc-baffles. In *Eighth International Congress of Fluid Dynamics & Propulsion 2006*, December, pp. 14-17.

Eiamsa-ard, S., Wongcharee, K., Eiamsa-Ard, P., & Thianpong, C. Heat transfer enhancement in a tube using delta-winglet twisted tape inserts. *Applied Thermal Engineering*, 2010, vol. 30, no. 4, pp. 310-318.

Fan, A. W., Deng, J. J., Nakayama, A., & Liu, W. Parametric study on turbulent heat transfer and flow characteristics in a circular tube fitted with louvered strip inserts. *International Journal of Heat and Mass Transfer*, 2012, vol.55, pp. 5205-5213.

Huang, T. S., Wang, P. H., CHIU, Y., & Jang, J. Y. Heat and fluid flow analysis over different tube inserts of recuperator. *China Steel Technical Report*, 2008, vol. 21, pp. 67-76.

Hutton D. *Fundamentals of finite element analysis.* The McGraw Hill, 2004.

Hossain S., Deb U. K., Rahman K. A., The Enhancement of Heat Transfer in a Circular Tube with Insert and without Insert by Using the Finite Element Method, *BSME International Conference on Thermal Engineering*, *Procedia Engineering*, 2015, vol. 105, pp. 81-88.

<https://www.snexplores.org/article/explainer-how-heat-moves>.

<https://www.simscale.com/docs/simwiki/heat-transfer-thermal-analysis/what-is-heat-transfer/>.

<https://engineeringlibrary.org/reference/laminar-and-turbulent-fluid-flow-doe-handbook>.

<https://www.theengineerspost.com/types-of-heat-exchanger/>.

Kakaç, S., Bergles, A. E., & Mayinger, F. Heat exchangers: thermal-hydraulic fundamentals and design 1981.

Kundu, P. K., Ira M. Cohen, David R. Dowling. Fluid mechanics – 5th ed. 2012, Elsevier Inc.

Li, P., Liu, P., Liu, Z., & Liu, W. Experimental and numerical study on the heat transfer and flow performance for the circular tube fitted with drainage inserts. International Journal of Heat and Mass Transfer, 2017, vol. 107, pp. 686-696.

Liu, P., Zheng, N., Shan, F., Liu, Z., & Liu, W. An experimental and numerical study on the laminar heat transfer and flow characteristics of a circular tube fitted with multiple conical strips inserts. International Journal of Heat and Mass Transfer, 2018, vol. 117, pp. 691-709.

Liu, S., & Sakr, M. A comprehensive review on passive heat transfer enhancements in pipe exchangers. Renewable and sustainable energy reviews, 2013, vol.19, pp. 64-81.

Mizanuzzaman M., Jahan N., Ahmed A., Rahman S., Mahmud M. A., Experimental Study of Temperature Distribution in Turbulent Flow through Tubes with Longitudinal Perforated X-Shaped Inserts, International Journal of Emerging Technology and Advanced Engineering(IJETAE), 2013, vol. 3, no. 1, pp 24-30.

Meyer, J. P., & Abolarin, S. M. Heat transfer and pressure drop in the transitional flow regime for a smooth circular tube with twisted tape inserts and a square-edged inlet. International Journal of Heat and Mass Transfer, 2018, vol.117, pp. 11-29.

McDonough, J. M. Lectures in elementary fluid dynamics: physics, mathematics and applications, 2009.

Matani, A. G., & Choudhari, M. R. S. Analysis of Heat Transfer Augmentation in Tube Using Triangular Wavy Tape Inserts. International Journal of Engineering Research and General Science, 2015, vol. 3 no.3.

Okbaz, A., Pınarbaşı, A., Olcay, A. B., & Aksoy, M. H. An experimental, computational and flow visualization study on the air-side thermal and hydraulic performance of louvered fin and round tube heat exchangers. International Journal of heat and mass transfer, 2018, vol. 121, pp.153-169.

Patil, S. V., & Babu, P. V. Heat transfer augmentation in a circular tube and squareduct fitted with swirl flow generators: a review. International Journal of Chemical Engineering and Applications, 2011, vol. 2 no 5, pp. 326.

Peiro, J., & Sherwin, S. Methods and models. Handbook of Materials Modeling, 2005, vol. I.

Rohsenow, W. M., Hartnett, J. P., & Cho, Y. I. Handbook of heat transfer, 1998, Vol. 3 New York: McGraw-hill.

- Roslim, M. K., Hassan, S., & Tesfamichael, A. Experimental investigation on heat transfer enhancement by using porous twisted plate as an insert in a fitted tube. *ARP Journal of Engineering and Applied Sciences*, 2015, vol. 10, no. 21, pp. 10164-10168.
- Salam, B., Biswas, S., Saha, S., & Bhuiya, M. M. K. Heat transfer enhancement in a tube using rectangular-cut twisted tape insert. *Procedia Engineering*, 2013, vol. 56, pp. 96-103.
- Salman, S. D., Kadhum, A. A. H., Takriff, M. S., & Mohamad, A. B. Research Article CFD Analysis of Heat Transfer and Friction Factor Characteristics in a Circular Tube Fitted with Quadrant-Cut Twisted Tape Inserts 2013.
- Suwannapan, S., Skullong, S., & Promvong, P. Thermal characteristics in a heat exchanger tube fitted with zigzag-winglet perforated-tapes. *Journal of Research and Applications in Mechanical Engineering*, 2015, vol. 3, no. 1, pp. 29-36.
- Sadashiv, N. M. Numerical Simulation of Enhancement of Heat Transfer in a Tube with And without Rod Helical tape Swirl Generators. *International journal of research in aeronautical and mechanical engineering*, 2014, vol. 2, no. 1, pp. 112-128.
- Saha, S. K., Gaitonde, U. N., & Date, A. W. Heat transfer and pressure drop characteristics of laminar flow in a circular tube fitted with regularly spaced twisted-tape elements. *Experimental Thermal and Fluid Science*, 1989, vol. 2, no 3, pp. 310-322.
- Tabatabaeikia, S., Mohammed, H. A., Nik-Ghazali, N., & Shahizare, B. (2014). Heat transfer enhancement by using different types of inserts. *Advances in Mechanical Engineering*, 2014, vol. 6, pp. 250354.
- Tam, L. M., & Ghajar, A. J. Transitional heat transfer in plain horizontal tubes. *Heat Transfer Engineering*, 2006, vol. 27, no. 5, pp. 23-38.
- Yaningsih, I., & Wijayanta, A. T. Influences of pitch-length louvered strip insert on thermal characteristic in concentric pipe heat exchanger. In *MATEC Web of Conferences EDP Sciences* 2017, Vol. 101, pp. 03014.
- Yadav, A. P., Pranit, M., & Patil, P. A. The Effect of insertion of different geometries on heat transfer performance in circular pipe-a review. *International Journal of Modern Engineering Research*, 2014, vol. 4, no. 11, pp. 47-53.
- Yu, W. H., & Wiwatanapattaphee, B. *Finite Element Method and Application*, 2006.
- www.comsolmultiphysics.com.